

An aerial photograph of the University of Jyväskylä campus in Finland. The image shows several large, modern white buildings with flat roofs, situated along a river. A cable-stayed bridge crosses the river. In the background, a dense forest and a city skyline are visible under a clear sky.

Mass spectrometry and a study of Ag isotopes at the IGISOL facility

Lecture 5

Iain Moore (iain.d.moore@jyu.fi)

Department of Physics,
University of Jyväskylä, Finland



Outline of lecture 5



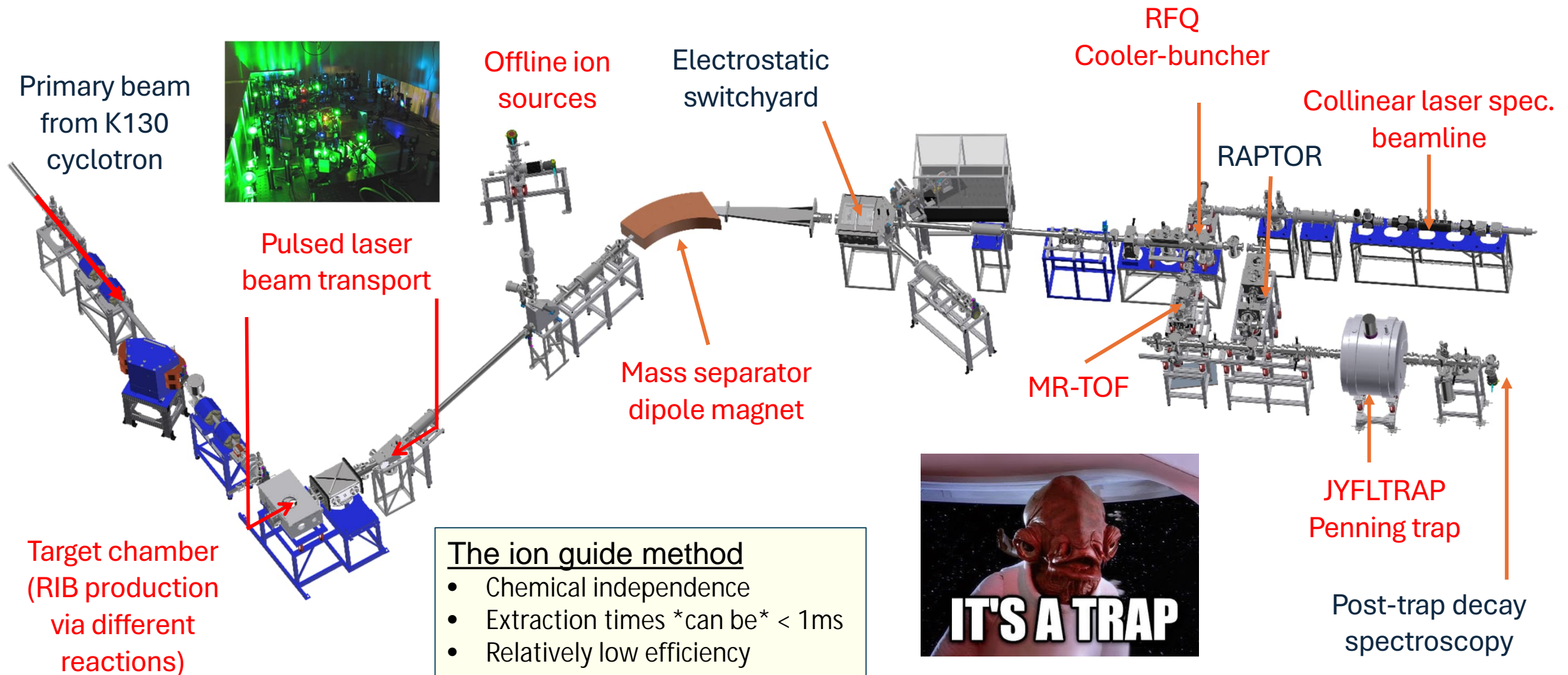
UNIVERSITY OF JYVÄSKYLÄ

- The IGISOL facility
- Ion manipulation: cooling and bunching
- The MR-TOF and Penning trap devices
- The study of silver – combining all our tools so far!*

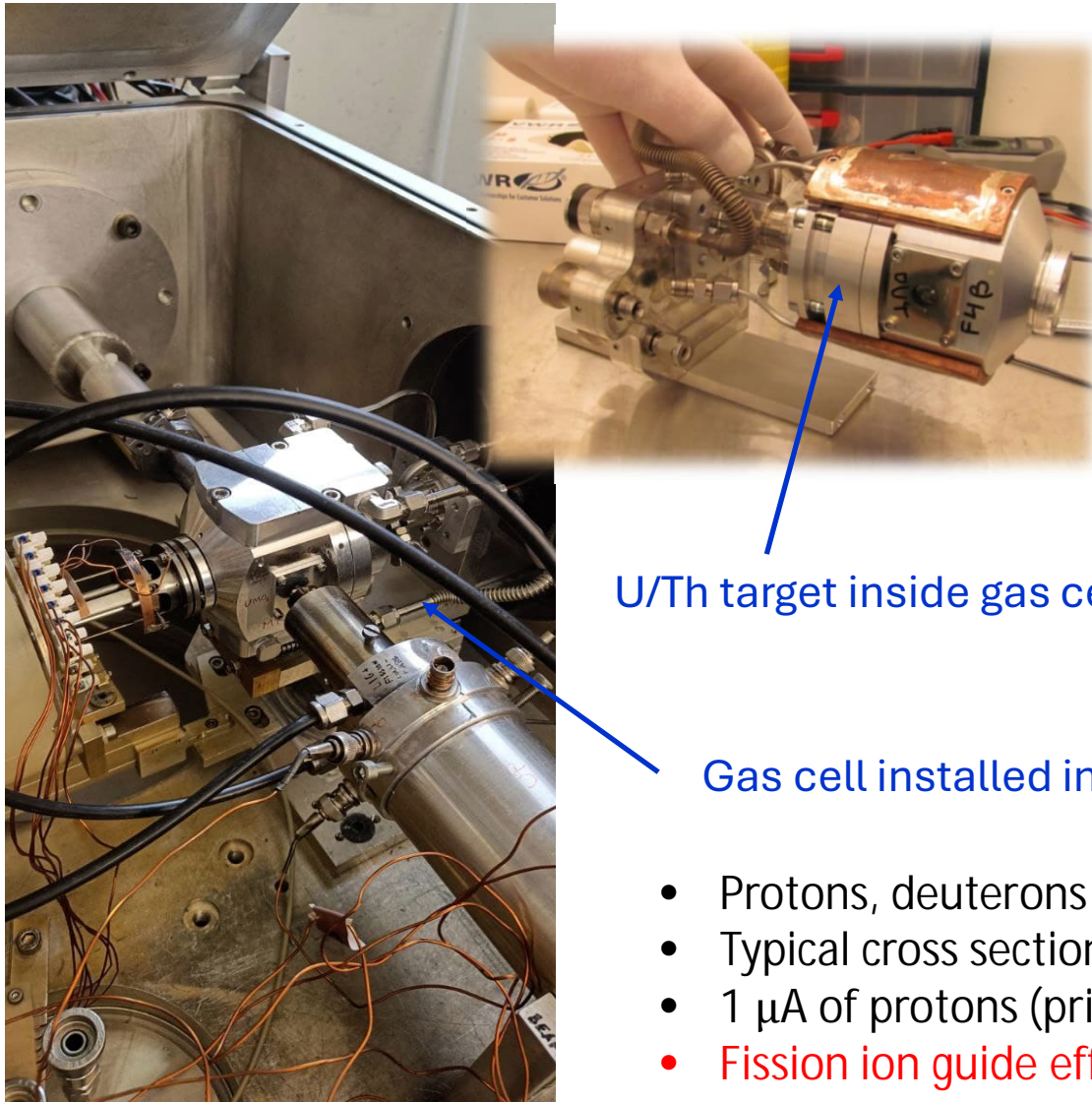
*Links to the discussion paper: Reponen *et al.*,
Nature Comm. 12 (2021) 4596



The IGISOL radioactive beam facility

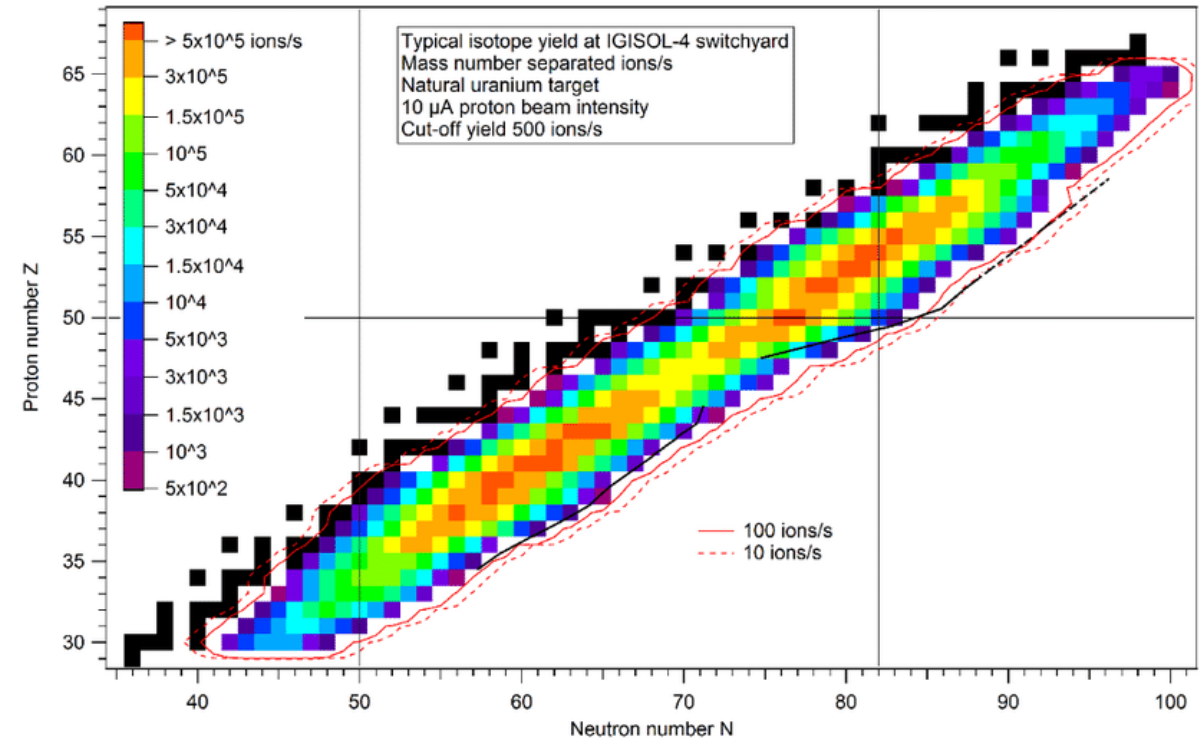


Production of neutron-rich isotopes



U/Th target inside gas cell

Gas cell installed into ``target chamber``

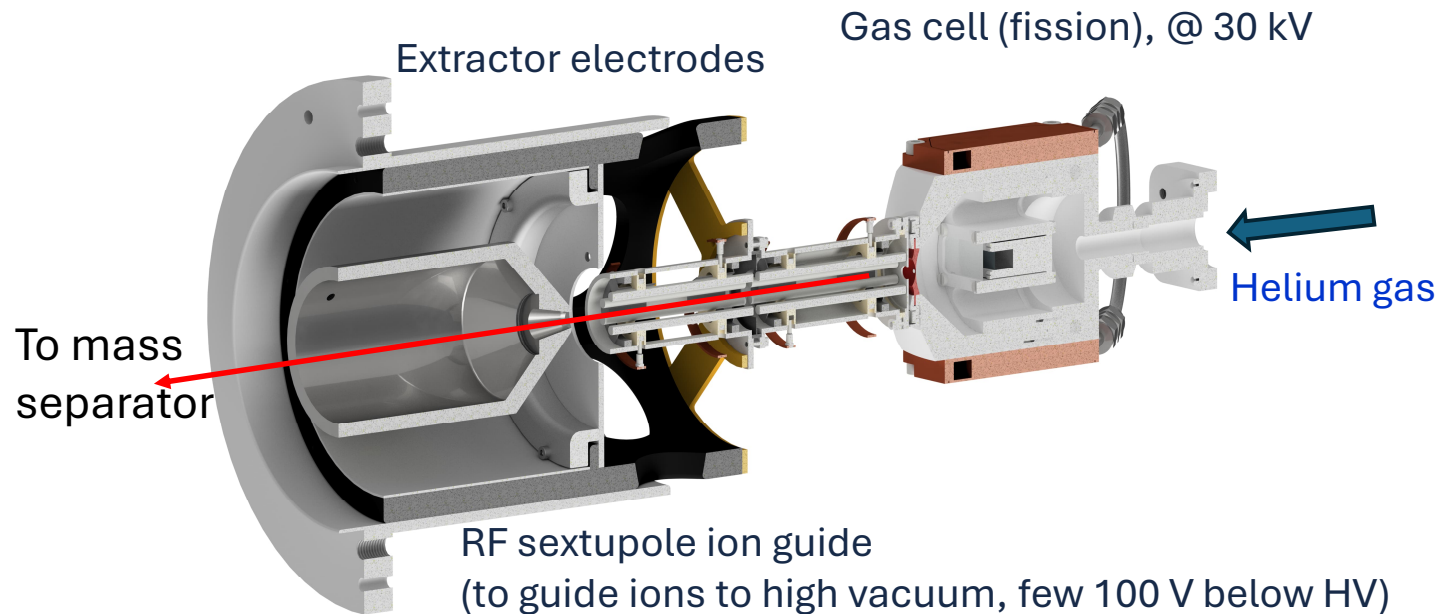


- Protons, deuterons on U/Th targets ($\sim 15 \text{ mg/cm}^2$)
- Typical cross section $\sim 1\text{-}1.5 \text{ barn}$ @ 30 MeV – note, this is a huge cross section!!
- 1 μ A of protons (primary beam) leads to 3×10^9 fissions/s (isotropically distributed)
- Fission ion guide efficiency $\sim 0.1\%$ (limited by stopping of fission fragments)

Extraction and acceleration of ions

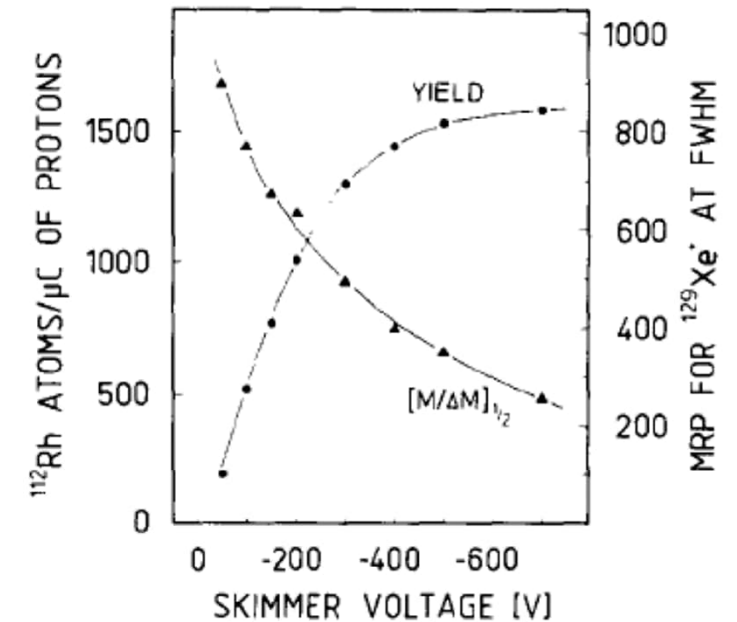
Typical ‘‘low-energy’’ ISOL/IGISOL beams are accelerated to 30-60 keV energy.

- Too high energy requires high/ultrahigh vacuum; discharging, inconvenient!
- Too low energy, more difficult to transport ion beam with electrostatic elements.
- Too low energy: typical dipole magnets suffer from poor mass resolution.



High vacuum region
($\sim 10^{-6}$ mbar)

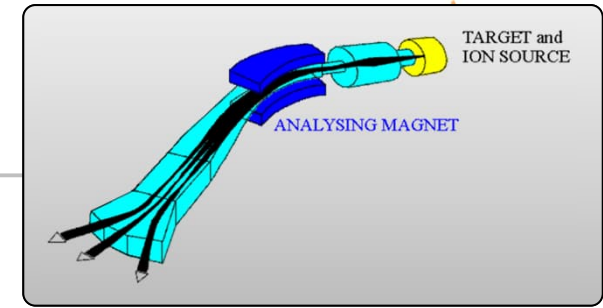
Poor vacuum ($\sim 10^{-2,-1}$ mbar)



P. Taskinen et al., NIMA 281 (1989) 539

- Mass resolving power & yield were seen to depend sensitively on V_{sk}
- This led to an ion beam energy spread (10 – 150 eV).

First stage of mass separation



We saw that in Lecture 2, radioactive beams are often severely contaminated!!



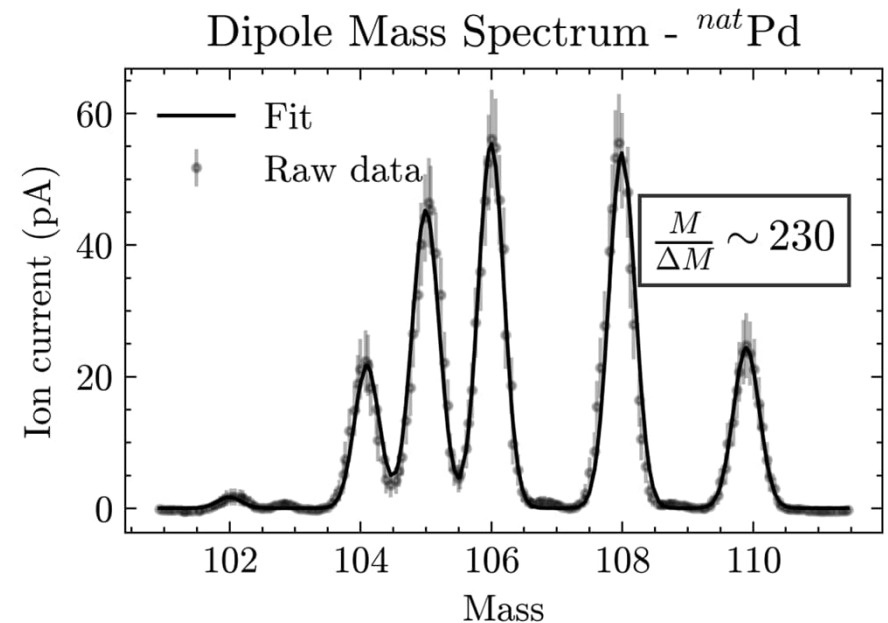
Most ISOL facilities will have an isotope separator. At IGISOL, after acceleration of the ion beam we pass through a dipole sector magnet. Other facilities may use two (e.g., ISOLDE...)

Mass Resolving Power

$$R = \frac{M}{\Delta M} \quad (\text{at full-width half-maximum})$$

The bigger the number the better!

The experimental mass resolving power is affected by the energy spread and emittance (or quality) of the ion beam.



Note: isotopic abundance of ^{102}Pd ~1%

Limitations with the dipole mass separator

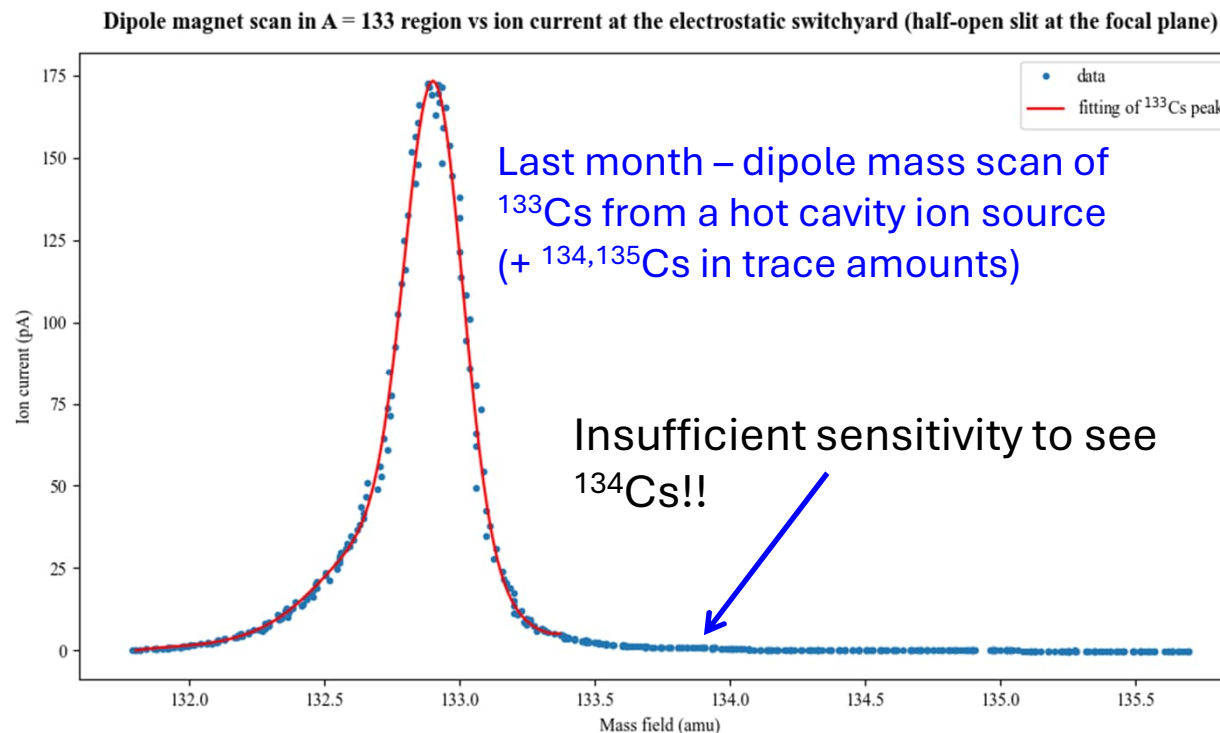
Well, obviously the mass resolving power!

^{106}Cd	^{107}Cd	^{108}Cd	^{109}Cd
^{105}Ag	^{106}Ag	^{107}Ag	^{108}Ag
^{104}Pd	^{105}Pd	^{106}Pd	^{107}Pd
^{103}Rh	^{104}Rh	^{105}Rh	^{106}Rh

Isotopes – MRP required to separate (^{105}Pd , ^{106}Pd) ~ 100

Isobars – MRP required to separate (^{106}Ag , ^{106}Pd) ~ 33000

Isomers – MRP required to separate (^{106}Ag , $^{106\text{m}}\text{Ag}$) ~ 110000



- Mass peak tailing towards lower masses – could be effect of energy spread
- If we move to single-ion counting detector, we start to saturate due to the tail of ^{133}Cs

Why would we wish to bunch an ion beam?

Our ``low-energy`` ISOL/IGISOL beams are typically continuous (unless we apply some form of bunched release at the source). Many experiments however require cooled and bunched beams.

- Low energy spread:
 - Collinear laser spectroscopy
 - Velocity spread \rightarrow Doppler broadening

- Low temporal spread
 - Multi-Reflection Time-of-Flight Mass Spectrometer (MR-TOF)

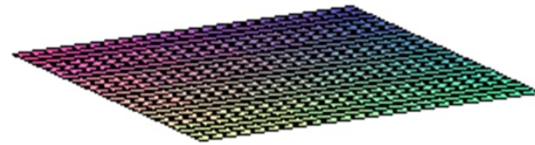
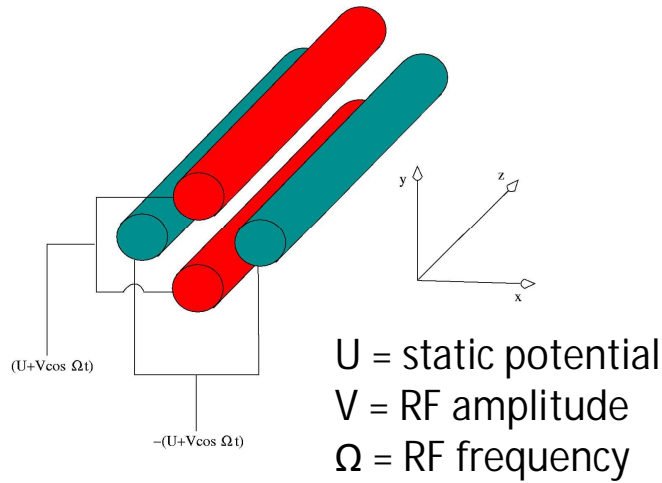
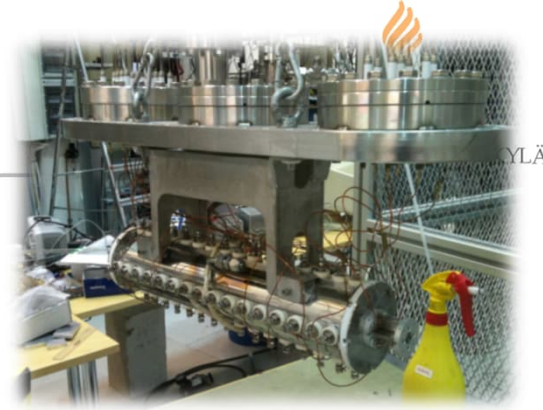
- Simply storing:
 - Wait for decay

		Ground state
Isomeric state	<div data-bbox="338 1049 611 1118"> <div>54</div> <div>27</div> <div>Co</div> <div>27</div> </div> <div data-bbox="338 1118 611 1252"> <div>1.48 m 7⁺ T=0</div> <div>E_{ex} 197.57 (0.10)</div> <div>β⁺=100%</div> </div>	<div data-bbox="611 1049 817 1118"> <div></div> <div></div> <div></div> </div> <div data-bbox="611 1118 817 1252"> <div>193.28 ms 0⁺ T=1</div> <div>M⁻ 48010.0 (0.4)</div> <div>β⁺=100%</div> </div>

- Bunched beam
 - Transfer to other experiments that have no cooling possibility or low continuous beam capture efficiency
 - Penning traps
 - Electron beam ion traps
 - Pulsed drift tubes
 - Decay spectroscopy requiring clear $t=0$
 - Collinear laser spectroscopy
 - Signal-to-background improvement $> 10^4$ (seen in Lecture 3)

The radiofrequency quadrupole / Paul trap

Three-dimensional confinement of ions can be achieved in a linear RF quadrupole structure by segmenting four rods and applying appropriate dc potentials to the segments.



- Equations of motion (Mathieu equations) can be found in textbooks
- Radiofrequency, time-varying electric field required to confine ions. Time-average force towards the central axis.
- ~1 MHz, 500 Vpp

Cooling of the ions means to reduce their motional amplitudes.

- Overall: beam emittance reduction
- Emittance: transverse phase space “size”, unit: π mm mrad at kinetic energy X
- Many other methods of cooling (radiative, resistive, evaporative, laser...)

Buffer gas / collisional cooling

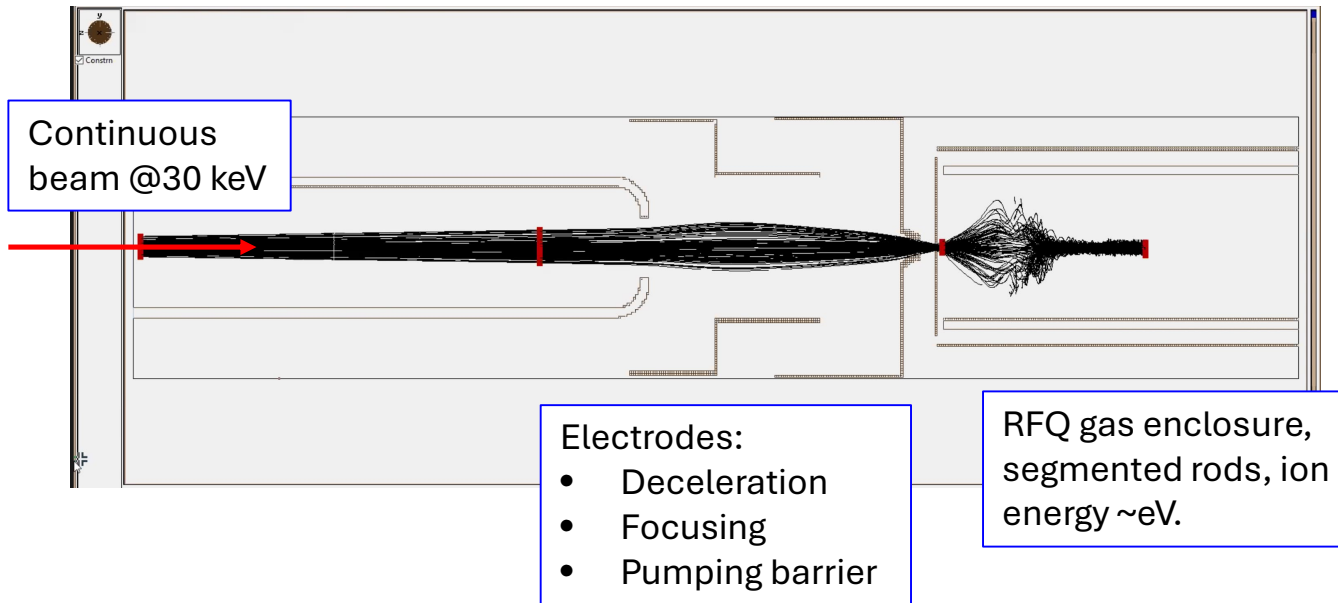
- The most versatile and important method in eV range
- Neutral gas molecules collide with ions (He, Ne, Ar...)
- The cooling limit is the buffer gas temperature (often at room temperature). Thermal motion remains.

Many excellent reviews discuss these aspects in detail:

K. Blaum, High accuracy mass spectrometry with ions, Phys. Rep. 425 (2006) 1

The JYFL gas-filled RFQ

Injection of ions into the RFQ

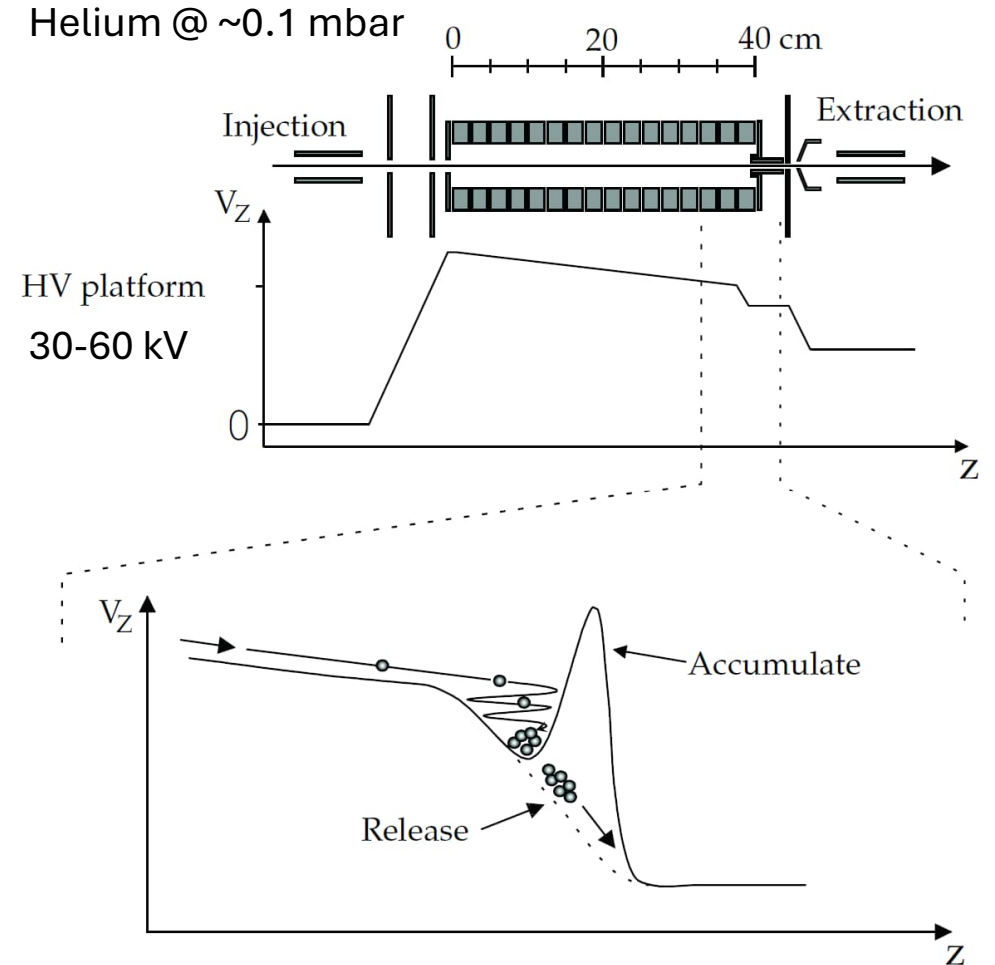


• Incoming beam:

- ~10 eV energy spread
- 15π mm mrad
- Continuous beam

Outgoing beam:

- ~1 eV energy spread
- 3π mm mrad (at 30 keV)
- Bunched beam $\Delta t \sim 5 \mu\text{s}$
- Transmission ~60-70%



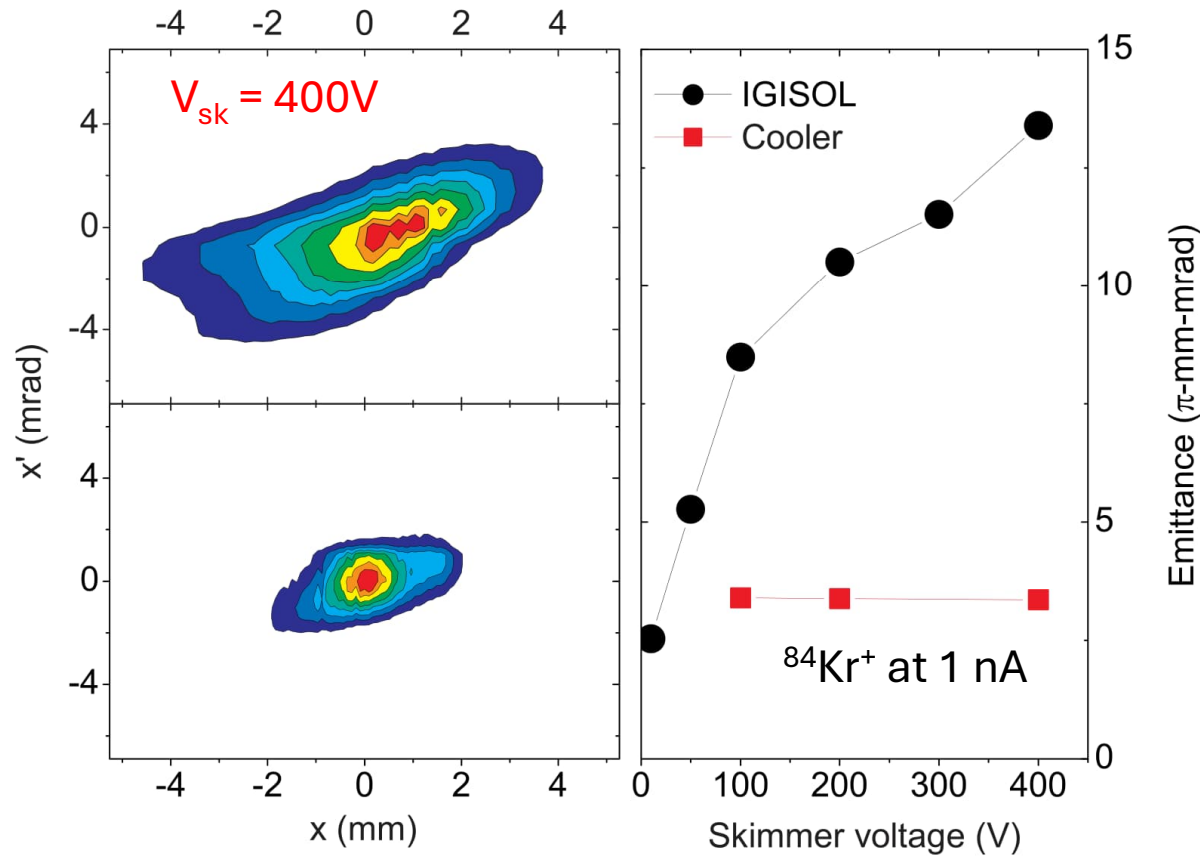
A. Nieminen et al., Nucl. Instr. and Meth. A 469 (2001) 244

Benefits: the beam has its memory erased ☺



UNIVERSITY OF JYVÄSKYLÄ

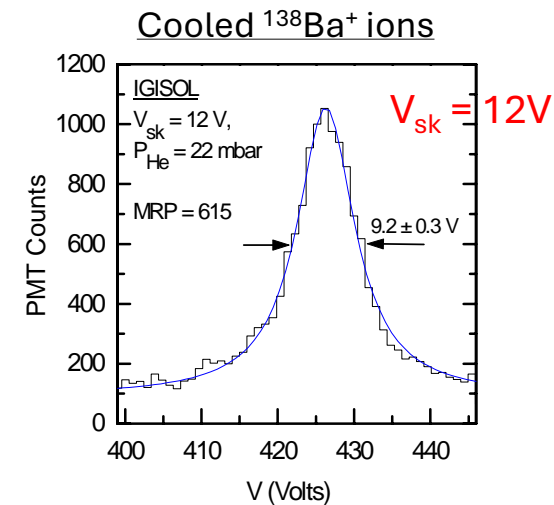
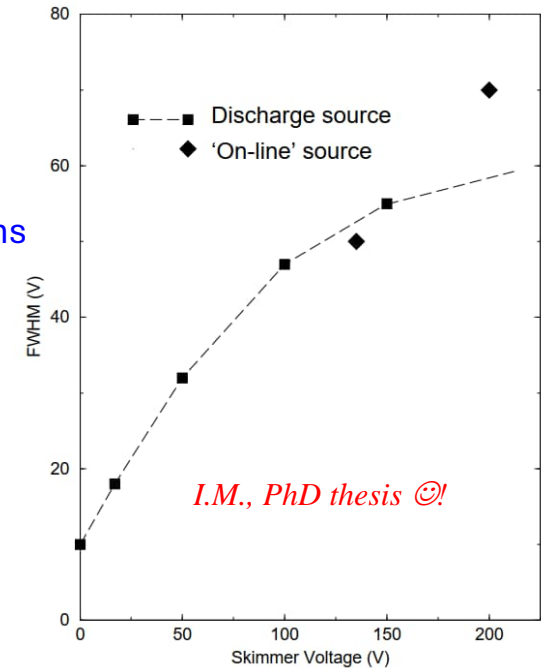
Beam emittance (quality of the beam) before and after the cooler-buncher



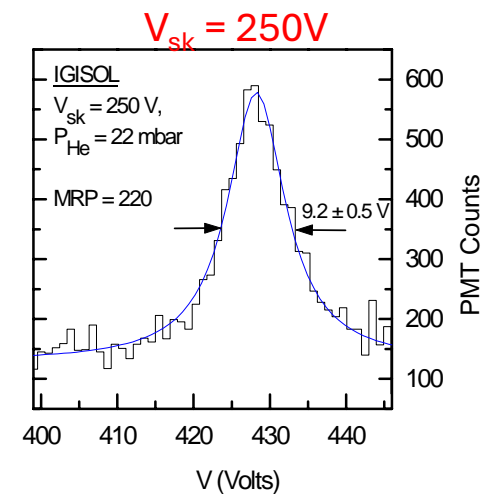
A. Nieminen et al., Nucl. Instr. and Meth. B 204 (2003) 563

Recall, as V_{sk} increases, the energy spread ΔE also increases!

Laser resonance of Ar^+ ions as a function of V_{sk}

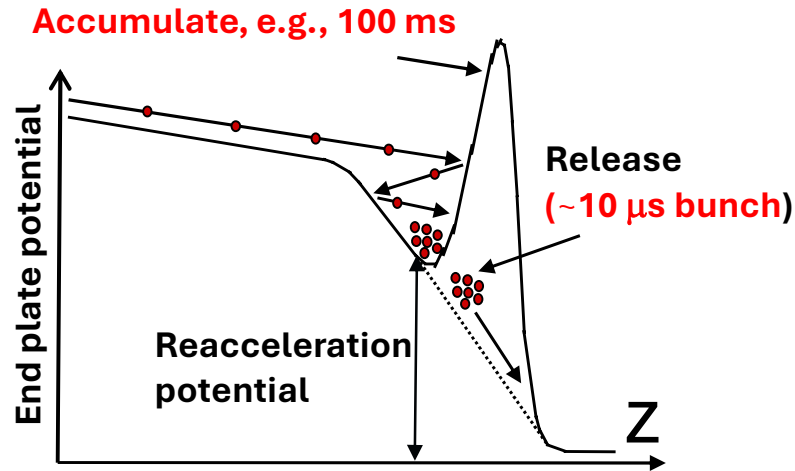


- Two skimmer voltages used
- Post-cooler, no change in spectral line profile seen.

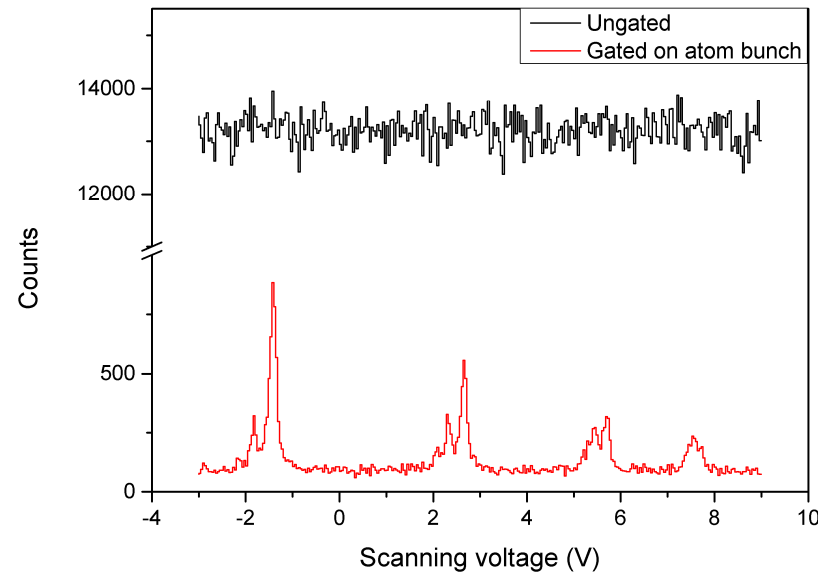


Towards time-focused bunching

Recall from Lecture 3: application of bunching for laser spectroscopy.



P. Campbell et al., PRL 89 (2002) 082501



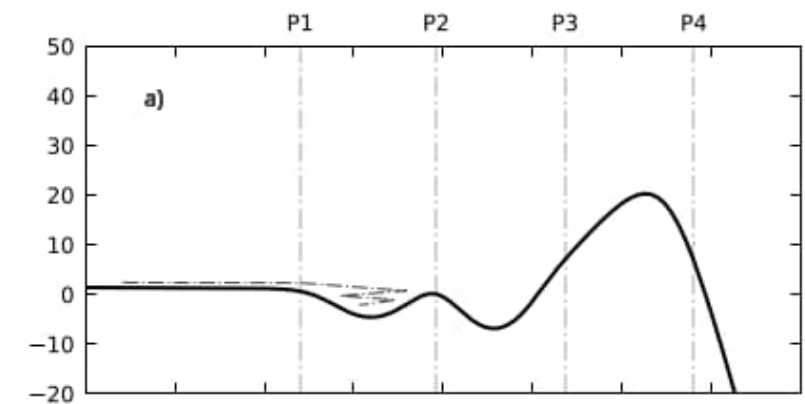
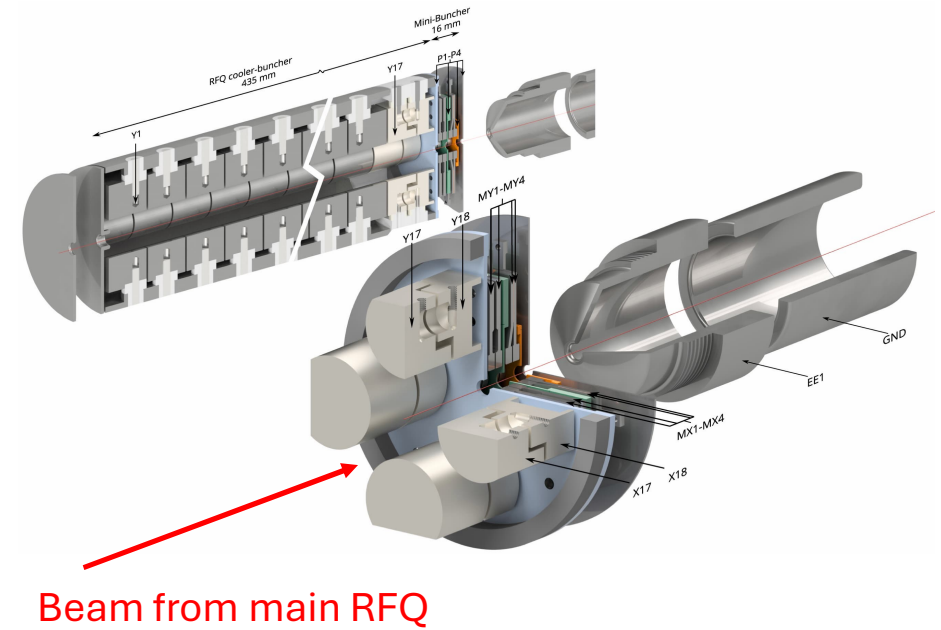
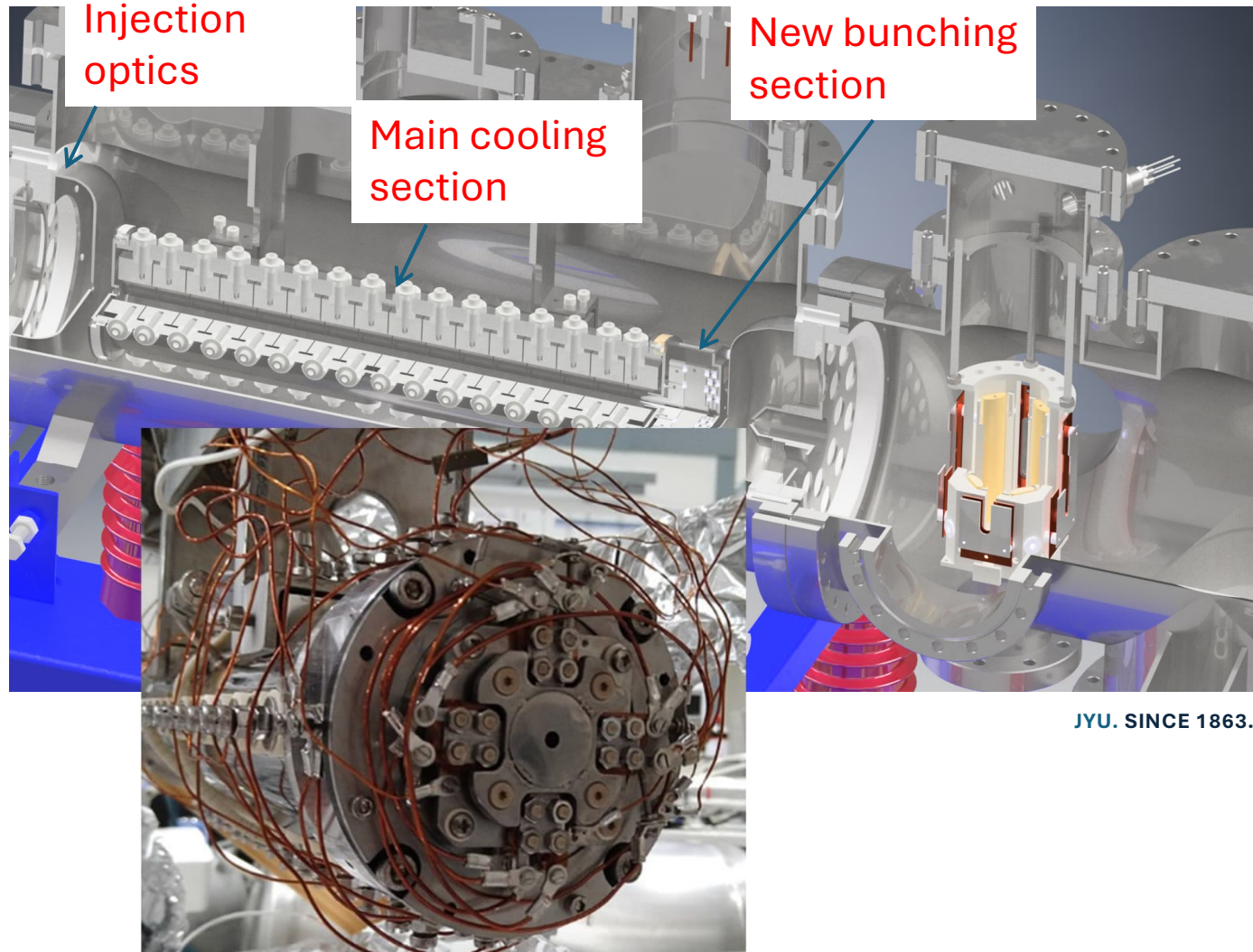
- Typical bunched widths from ~1 – 10 μs
- Bunching times: 1 ms to >100 ms depending on experimental requirements

For some applications, e.g., an MR-TOF mass spectrometer, the mass resolving power is determined by the minimum width of an ion bunch from the RFQ. Typically the demand is for <100 ns bunches.

$$\text{Background suppression} = \frac{\text{e.g., 100ms accumulation}}{10\mu\text{s gate width}} \sim 10^4$$

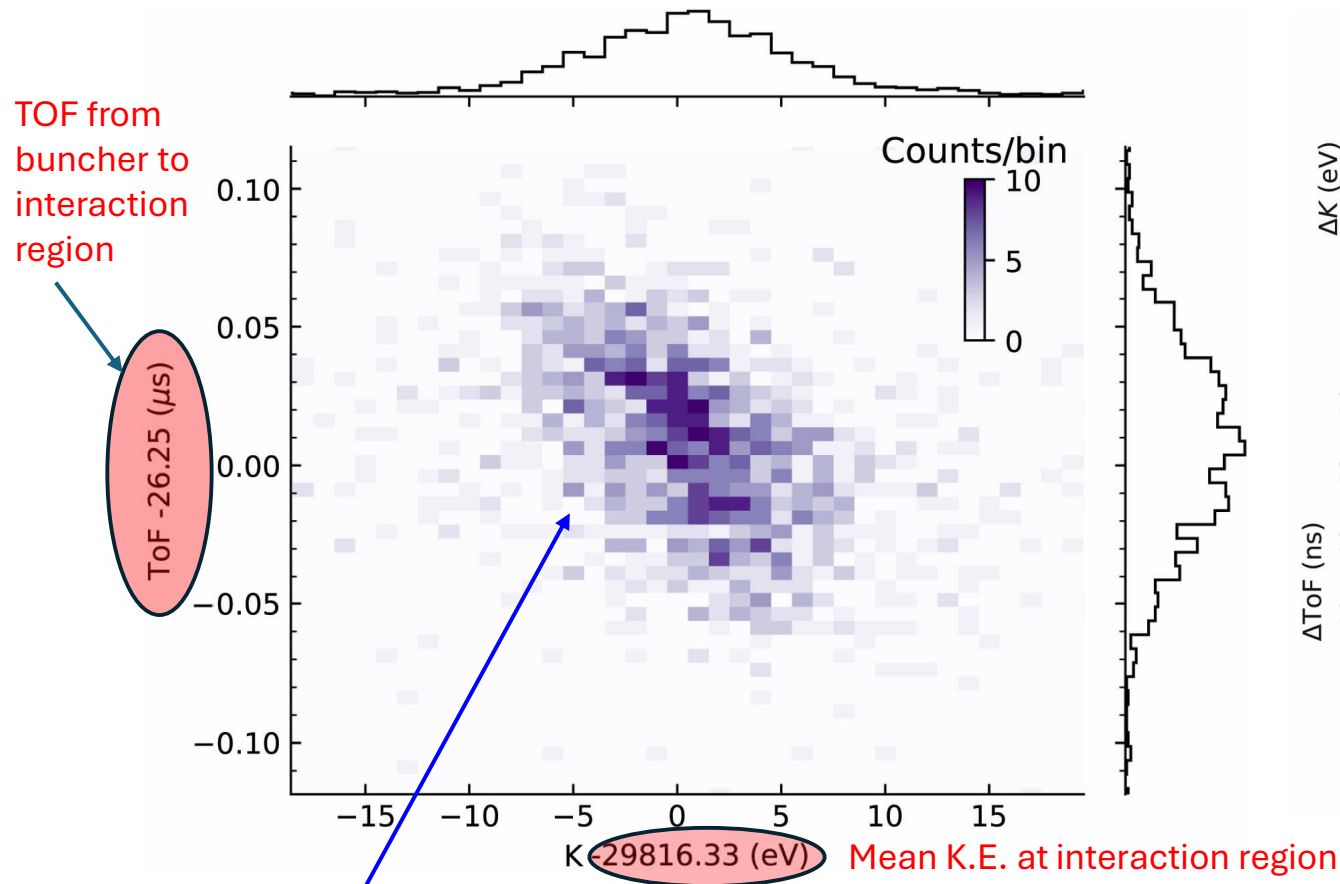
$$R = \frac{M}{\Delta M} = \frac{t_{\text{tof}}}{2\Delta t_{\text{tof}}}$$

A mini-buncher extension to the RFQ

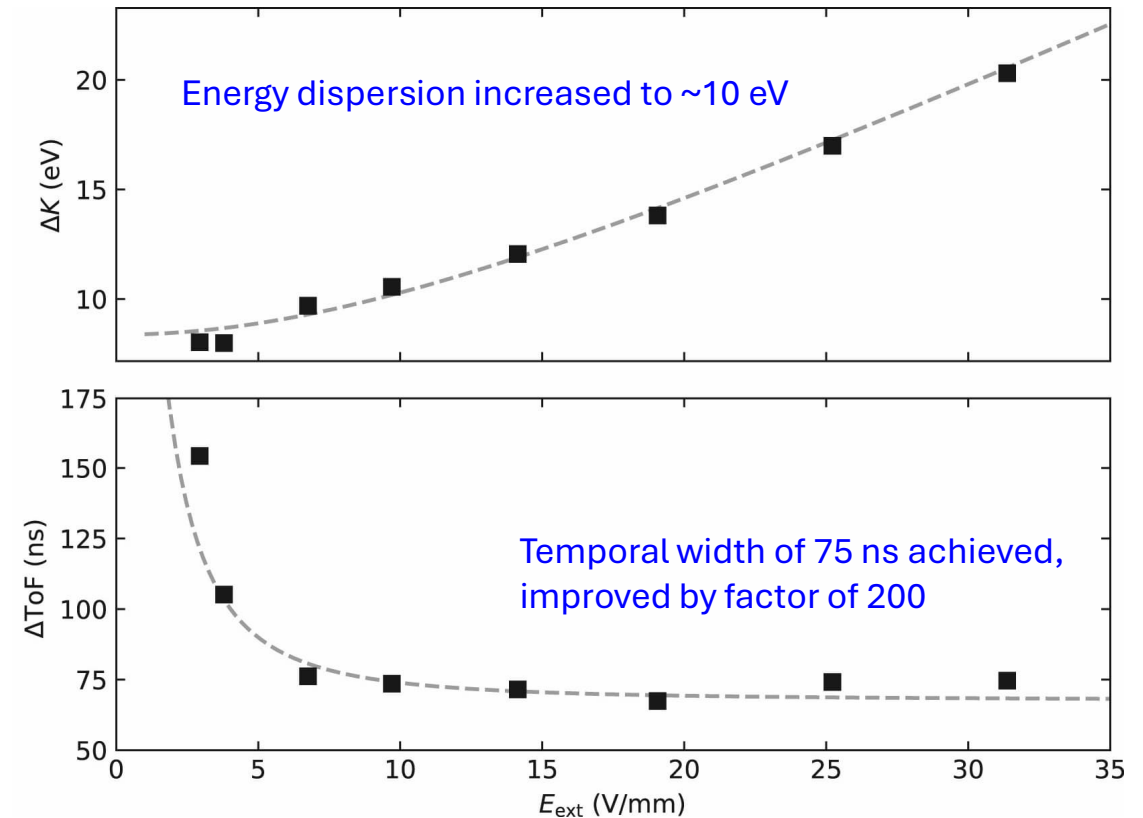


Determination of energy and temporal spread

Collinear laser spectroscopy of Sc^+ ions for different extraction fields from the mini-buncher.



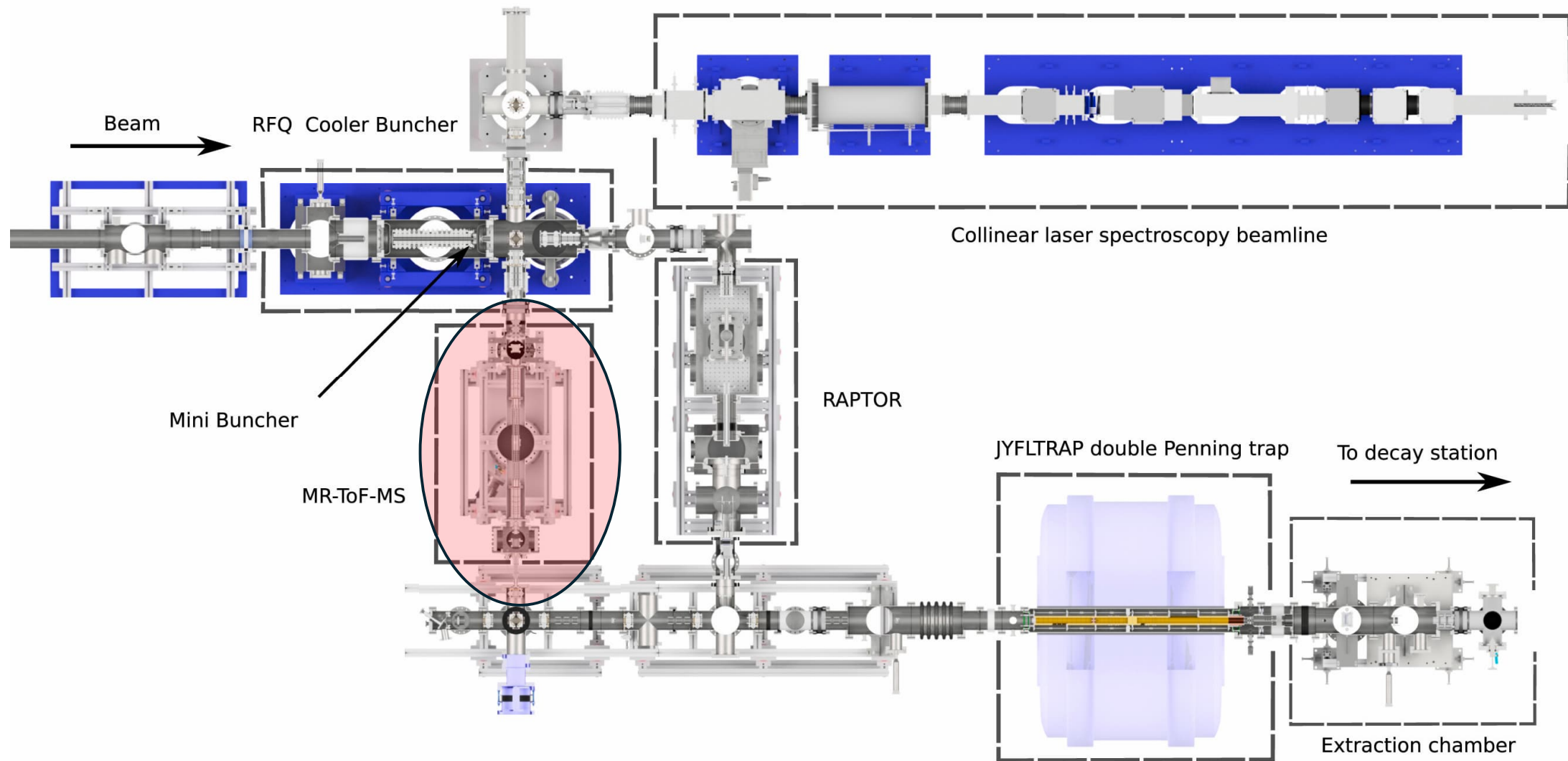
- Ellipsoid indicates the bunch has passed its time focus



- Decreasing the time dispersion of the bunch increases the energy spread.

V. Virtanen et al., Nucl. Instr. and Meth. A 1072 (2025) 170186.

A brief refresher of our experimental stations



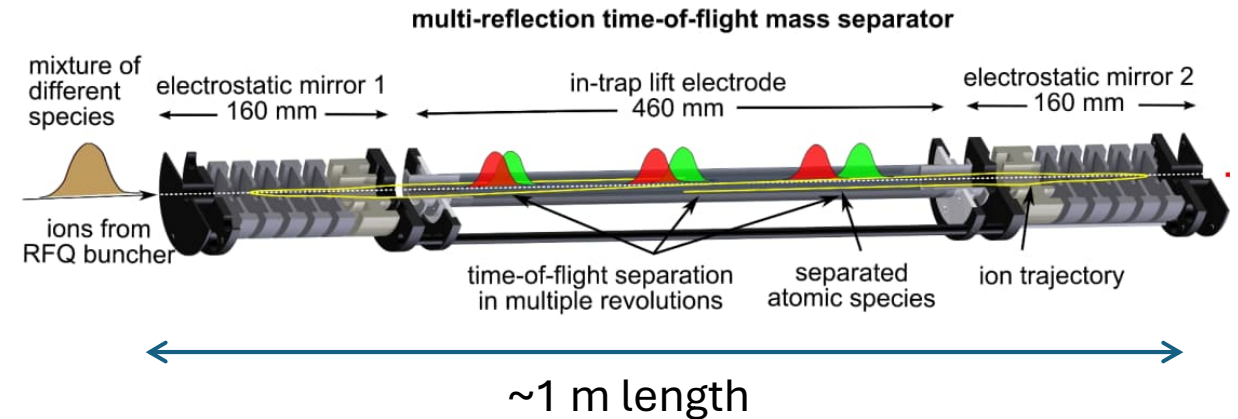
V. Virtanen et al., Nucl. Instr. and Meth. A 1072 (2025) 170186.

The MR-TOF mass spectrometer

Multi-reflection time-of-flight mass spectrometry

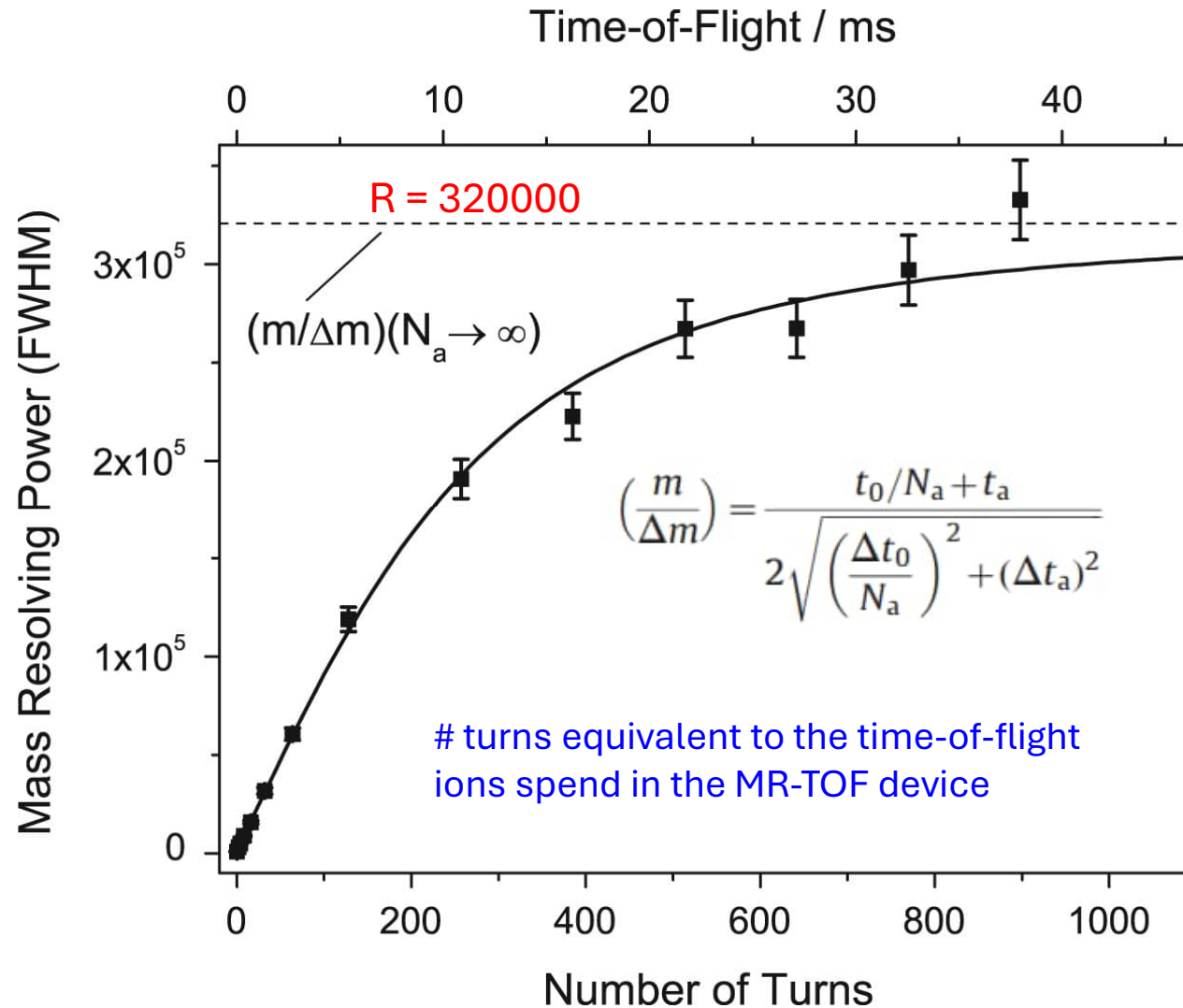
- Inject a bunch of ions into a device confined by electrostatic mirrors
- All ions have the same start time and kinetic energy (ideally)
- Let the ions bounce back and forth
- Separation with mass/charge ratio via time-of-flight (all ions move in a set potential)
- **More revolutions** = bigger time difference = better separation (= **better resolving power**)
- Extract ions towards a detector for time-of-flight measurement. **Mass separator** or **mass spectrometer**.

$$R = \frac{M}{\Delta M} = \frac{t_{tof}}{2\Delta t_{tof}}$$



- 100...10000x single TOF, up to ~100 ms, up to few km of flight path
- For nuclei with...
 - Short half-life (~ tens of ms)
 - Low production
- Non-scanning (this is a good thing!): measures the full mass spectrum simultaneously

Example of the mass resolving power



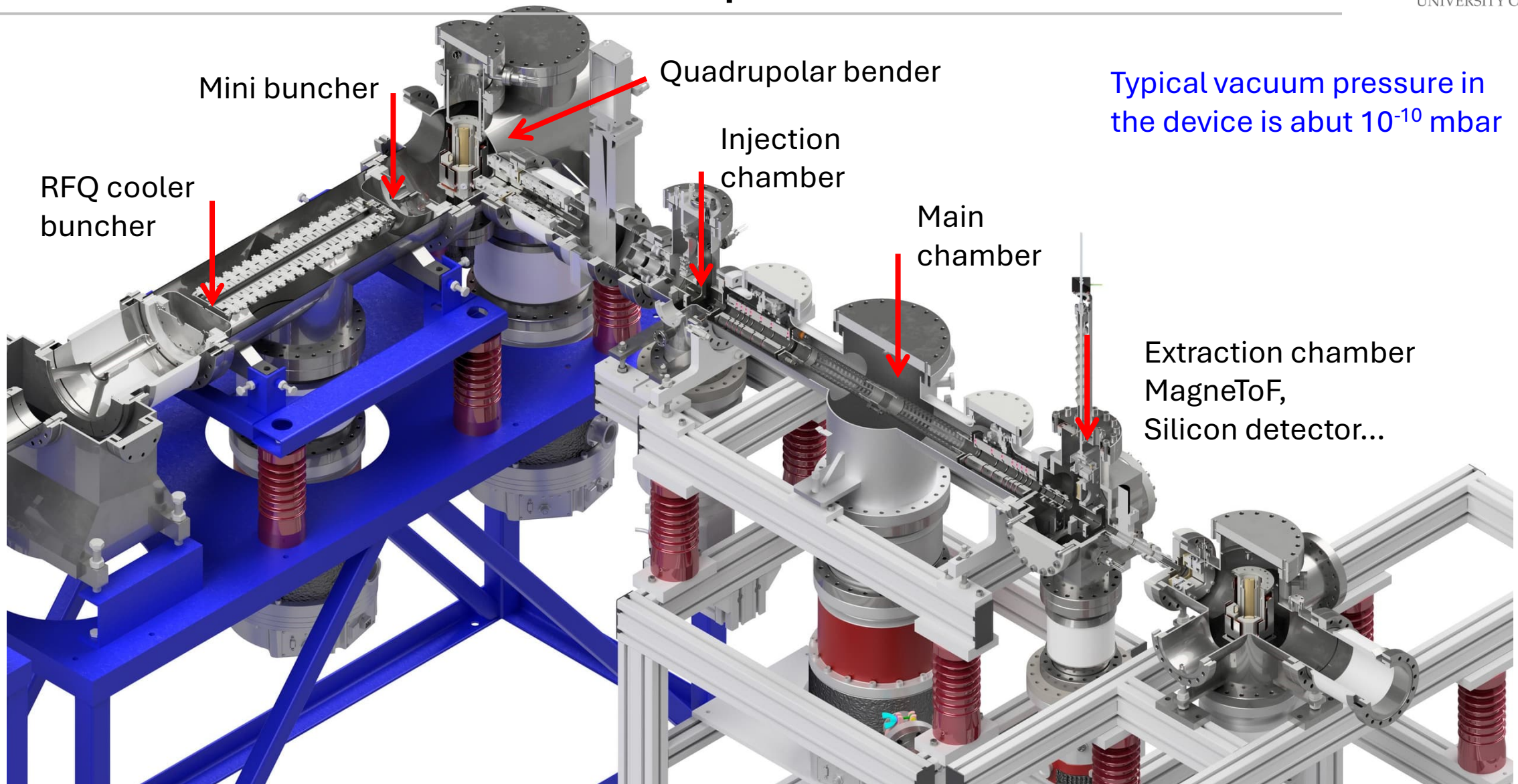
Example of MRP measured for $^{133}\text{Cs}^+$ with an MR-TOF-MS

- t_0 = TOF from start position to detector without any flight path extension
- t_a is the TOF for a single turn
- N_a is the number of passes in the device

$$R = \frac{M}{\Delta M} = \frac{t_a}{2\Delta t_a} \quad \dots \text{ as } N_a \rightarrow \infty$$

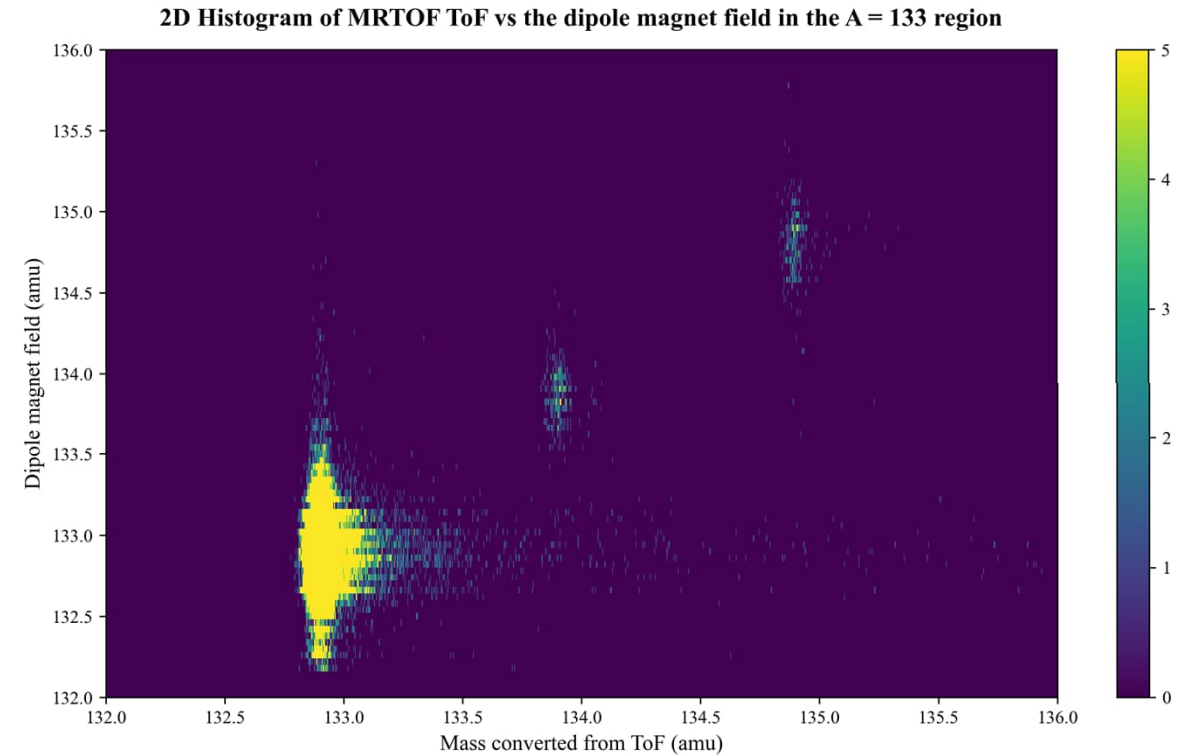
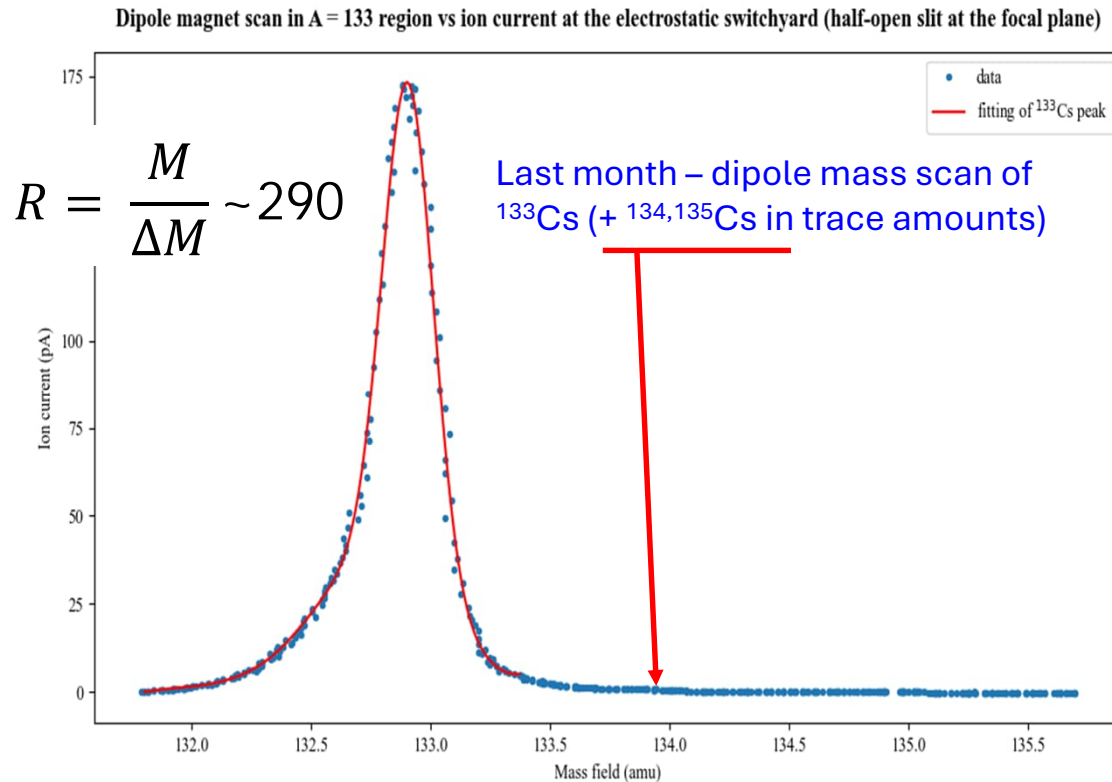
T. Dickel et al., Nucl. Instr. and Meth. A 777 (2015) 172

The IGISOL MR-TOF mass spectrometer



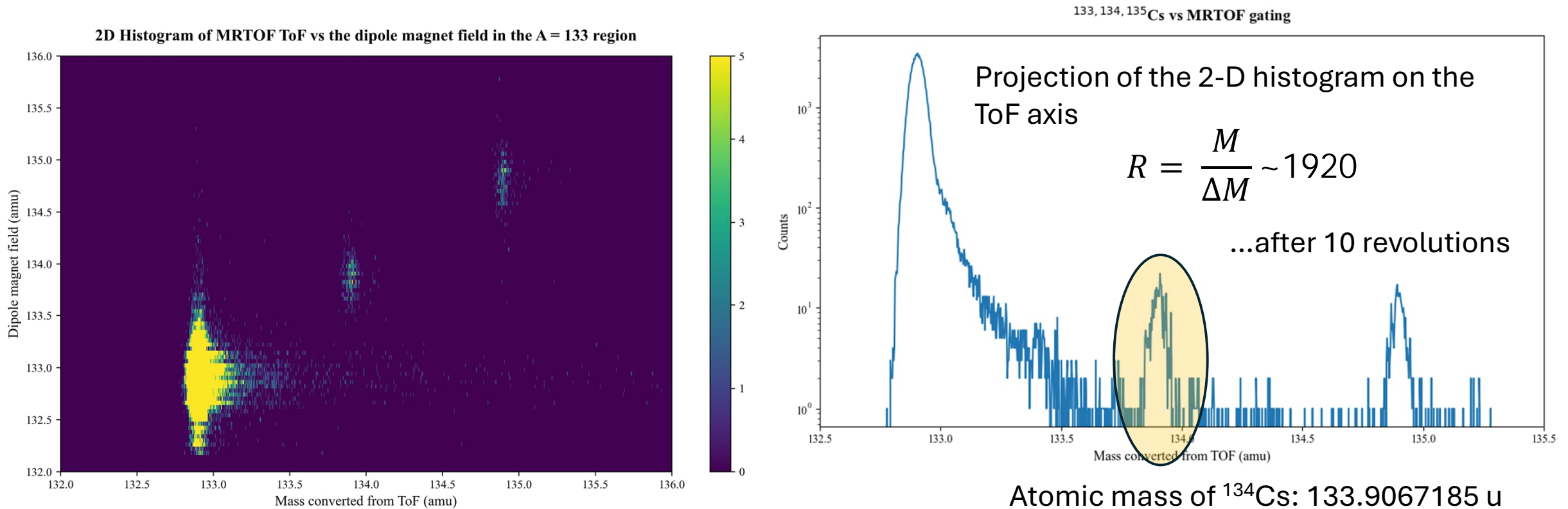
Exploiting the MR-TOF to identify $^{134,135}\text{Cs}^+$ ions

Remember I said we had insufficient sensitivity to see $^{134}\text{Cs}^+$...



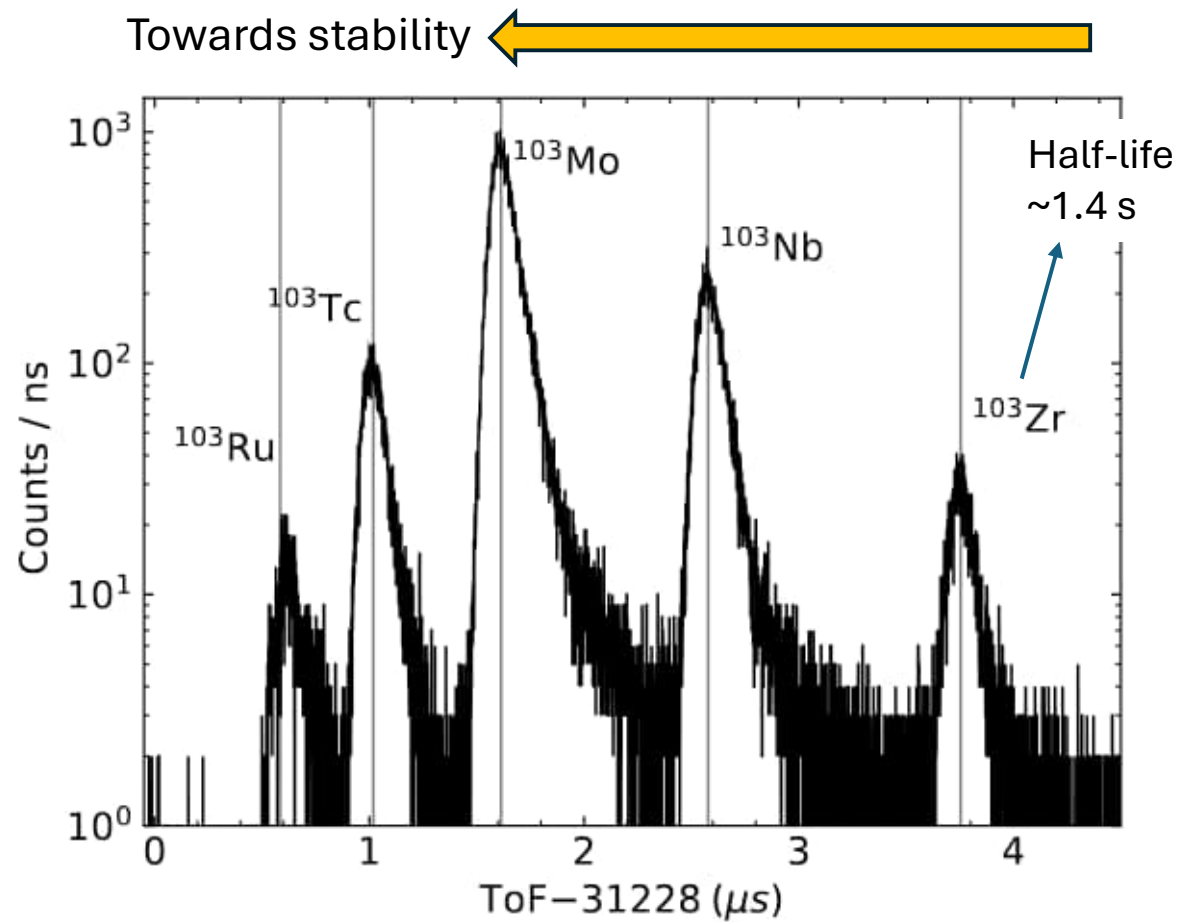
- After only 10 revolutions in the MR-TOF we could clearly separate out ^{133}Cs , ^{134}Cs and ^{135}Cs
- The only thing being scanned here is the magnetic field of the dipole magnet.

Exploiting the MR-TOF to identify $^{134,135}\text{Cs}^+$ ions



- By projecting the two-dimensional ion counts on the ToF axis, the peaks could be integrated to get the abundance ratio.
- Combine this ratio with gamma spectroscopy of ^{134}Cs we can estimate the activity when the sample was created.

MR-ToF: On-line mass spectra of fission fragments



$$R = \frac{t_a}{2\Delta t_a} \sim 10^5$$

Nucleus	103Rh	104Rh	105Rh	106Rh	107Rh	108Rh	109Rh
103Mo	STABLE	42.3 s	35.341 h	30.07 s	21.7 min	17 s	80.8 s
103Ru	STABLE	$\beta^- = 99.55\%$ $\alpha + \beta^- = 0.45\%$	$\beta^- = 100\%$	$\beta^- = 100\%$	$\beta^- = 100\%$	$\beta^- = 100\%$	$\beta^- = 100\%$
103Nb	STABLE	39.247 d	104Ru	105Ru	106Ru	107Ru	108Ru
103Zr	STABLE	31.55%	18.62%	4.44 h	371.8 d	3.73 min	4.55 min
103Y	STABLE	17.06%	$\beta^- = 100\%$	$\beta^- = 100\%$	$\beta^- = 100\%$	$\beta^- = 100\%$	$\beta^- = 100\%$
100Tc	101Tc	102Tc	103Tc	104Tc	105Tc	106Tc	107Tc
15.65 s	14.123 min	5.98 s	54.2 s	18.2 min	7.64 min	35.7 s	21.2 s
$\beta^- = 99.997\%$ $\alpha = 2.6e-3\%$	$\beta^- = 100\%$	$\beta^- = 100\%$	$\beta^- = 100\%$	$\beta^- = 100\%$	$\beta^- = 100\%$	$\beta^- = 100\%$	$\beta^- = 100\%$
99Mo	100Mo	101Mo	102Mo	103Mo	104Mo	105Mo	106Mo
65.936 h	7.07e+18 y	14.61 min	11.3 min	67.5 s	59.4 s	36.3 s	8.73 s
$\beta^- = 100\%$	9.744%	$\beta^- = 100\%$	$\beta^- = 100\%$	$\beta^- = 100\%$	$\beta^- = 100\%$	$\beta^- = 100\%$	$\beta^- = 100\%$
98Nb	99Nb	100Nb	101Nb	102Nb	103Nb	104Nb	105Nb
2.86 s	15 s	1.4 s	7.2 s	4.3 s	1.36 s	4.9 s	2.92 s
$\beta^- = 100\%$	$\beta^- = 100\%$	$\beta^- = 100\%$	$\beta^- = 100\%$	$\beta^- = 100\%$	$\beta^- = 100\%$	$\beta^- = 100\%$	$\beta^- = 100\%$
97Zr	98Zr	99Zr	100Zr	101Zr	102Zr	103Zr	104Zr
16.749 h	30.7 s	2.1 s	7.1 s	2.32 s	2.01 s	1.38 s	922 ms
$\beta^- = 100\%$	$\beta^- = 100\%$	$\beta^- = 100\%$	$\beta^- = 100\%$	$\beta^- = 100\%$	$\beta^- = 100\%$	$\beta^- = 100\%$	$\beta^- = 100\%$

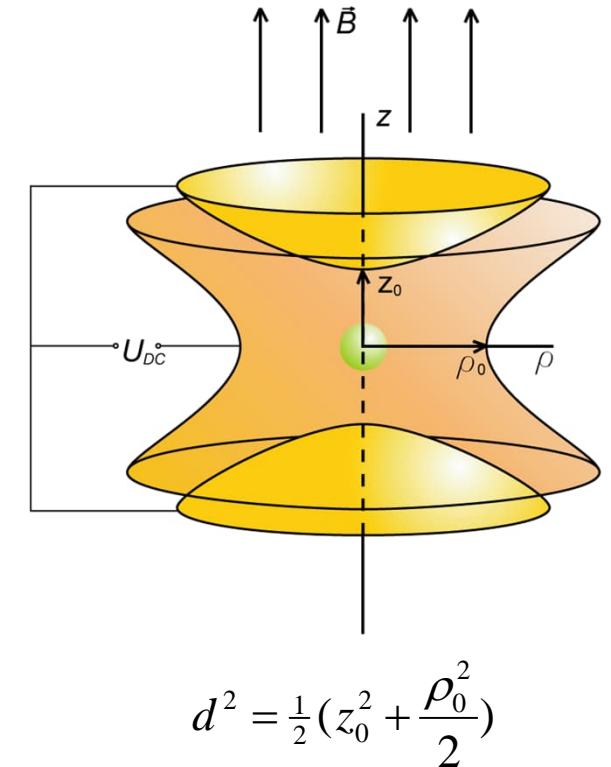
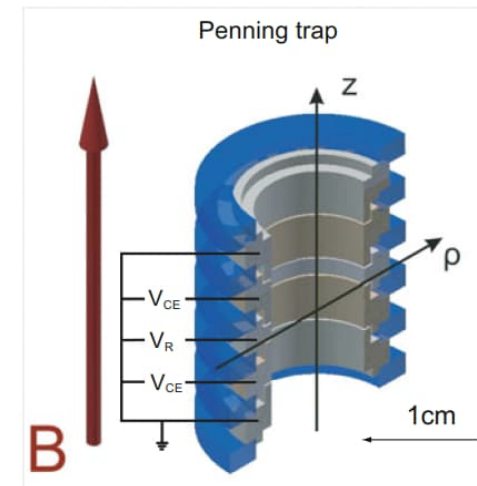
- Non-scanning method: stable & radioactive ions detected simultaneously

Typical mass precision: $\frac{\delta m}{m} \propto \frac{1}{R\sqrt{N}} \sim 10 \dots 100 \text{ keV}/c^2$

Penning trap mass spectrometry (PTMS)

As soon as masses of nuclides with half-lives longer than a few hundred ms have to be determined with a fractional uncertainty smaller than 10^{-7} – there is only one choice – Penning-trap mass spectrometry!

- Trapping of particle via motion in electro-magnetic field
- Strong homogeneous magnetic field in the z direction
- An ion with ratio q/m experiences a Lorentz force $\vec{F}_L = q\vec{v} \times \vec{B}$
- Weak quadrupole (harmonic) electrostatic potential
$$\phi(z, r) = \frac{U_{DC}}{2d^2} \left(z^2 - \frac{1}{2}\rho^2 \right)$$



Typical size a few cm

Ion motions in the Penning trap

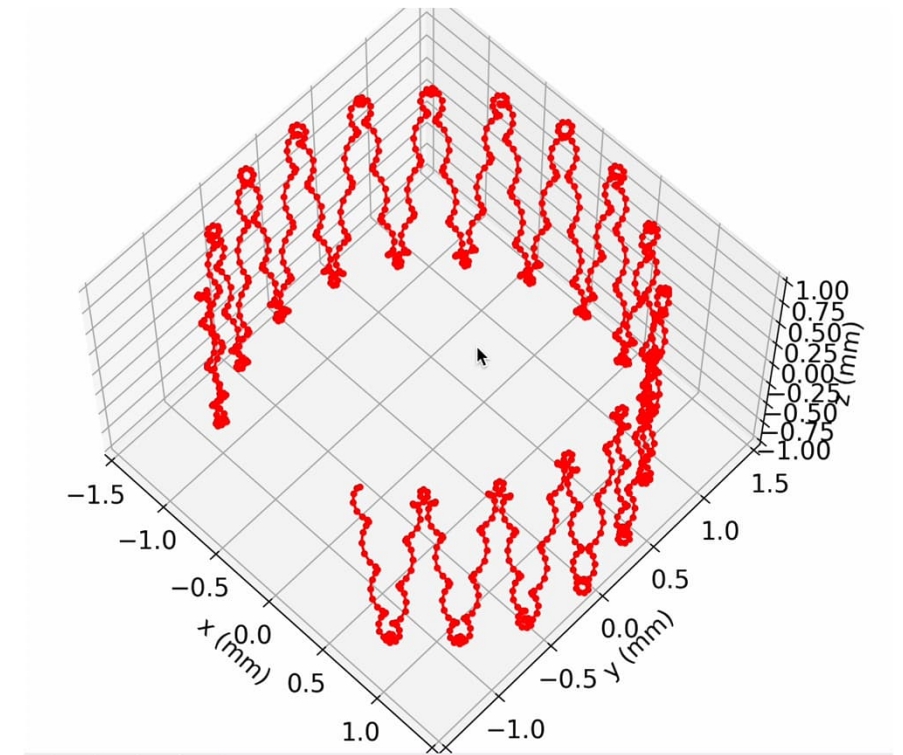
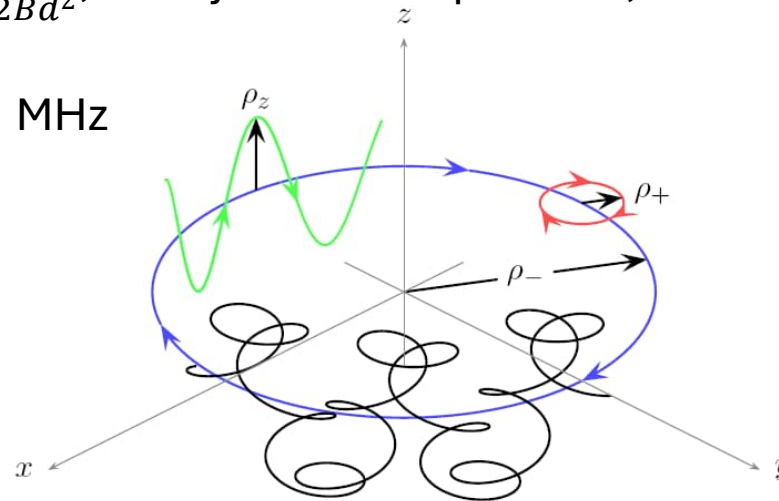
The trapped ion undergoes three motions – **cyclotron**, **magnetron** and **axial**, with frequencies ν_+ , ν_- and ν_z , respectively, which are uniquely determined by the trap parameters (B field, trapping potential and the trap dimension).

- Typical magnetic field for Penning traps for radioactive ions $\sim 7\text{T}$

$$\nu_z = \frac{1}{2\pi} \sqrt{\frac{qV_0}{md^2}}, \text{ harmonic oscillator, } \sim 20 \text{ kHz}$$

$$\nu_- = \frac{1}{4\pi} \left(\nu_c - \sqrt{\nu_c^2 - 2\nu_z^2} \right) \approx \frac{U}{2Bd^2}, \text{ nearly mass independent, } \sim 1 \text{ kHz}$$

$$\nu_+ = \frac{1}{4\pi} \left(\nu_c + \sqrt{\nu_c^2 - 2\nu_z^2} \right), \sim 1 \text{ MHz}$$



Penning trap ion manipulation techniques

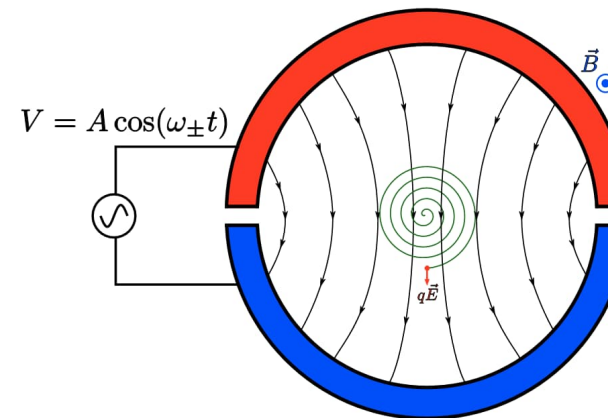
Here I will be extremely brief – sorry any trappers!! But there is a wealth of beautiful literature you can gorge yourselves on if you wish the juicy details!

Trap motion excitations

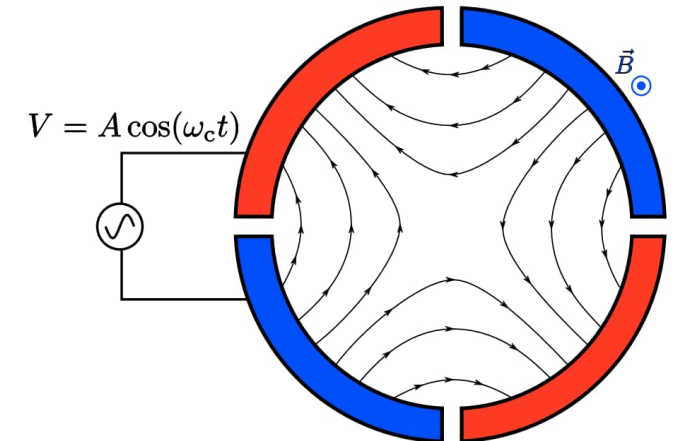
- We are interested in obtaining the atomic mass...the quantity for mass determination is:

$$\nu_c = \frac{1}{2\pi} \frac{q}{m} B$$

- For exotic nuclides, we get access to the cyclotron frequency by measuring the sideband frequency $\nu_+ + \nu_- = \nu_c$ (no need to measure axial frequency)



Dipole



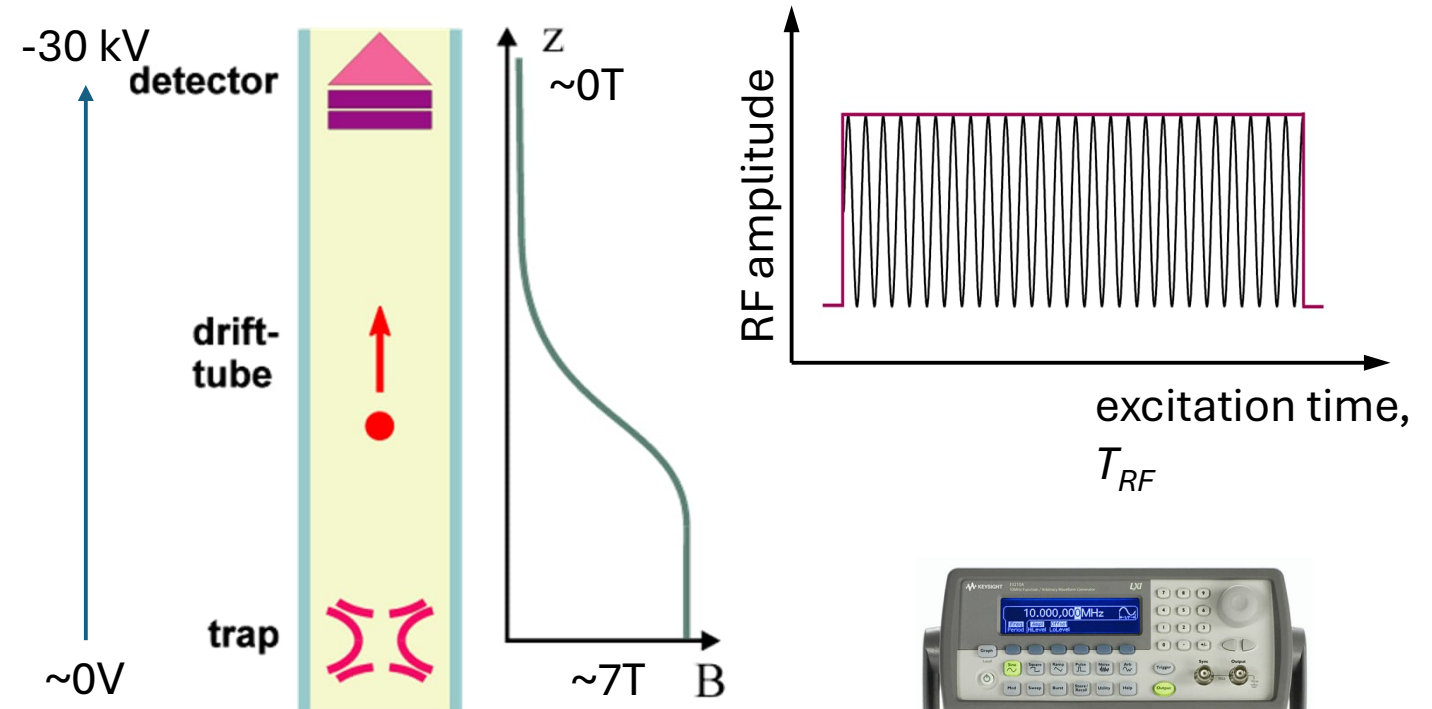
Quadrupole

- The ring electrode is split allowing for RF excitations to excite the (radial) motion amplitudes
- Eigenmotion excitation (**dipolar**)
- Conversions, coupling etc (**quadrupolar**)

Time-of-Flight Ion Cyclotron Resonance method

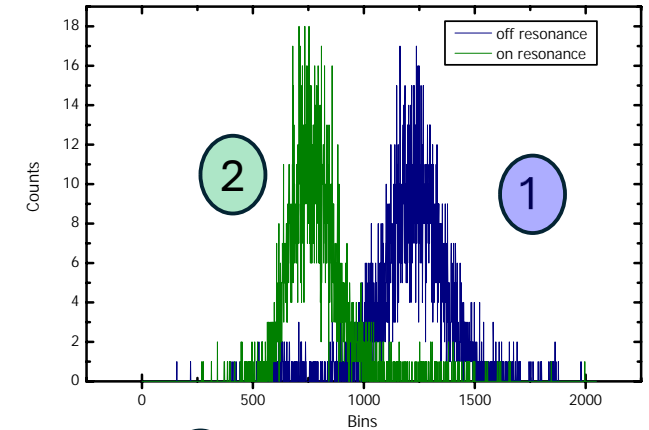
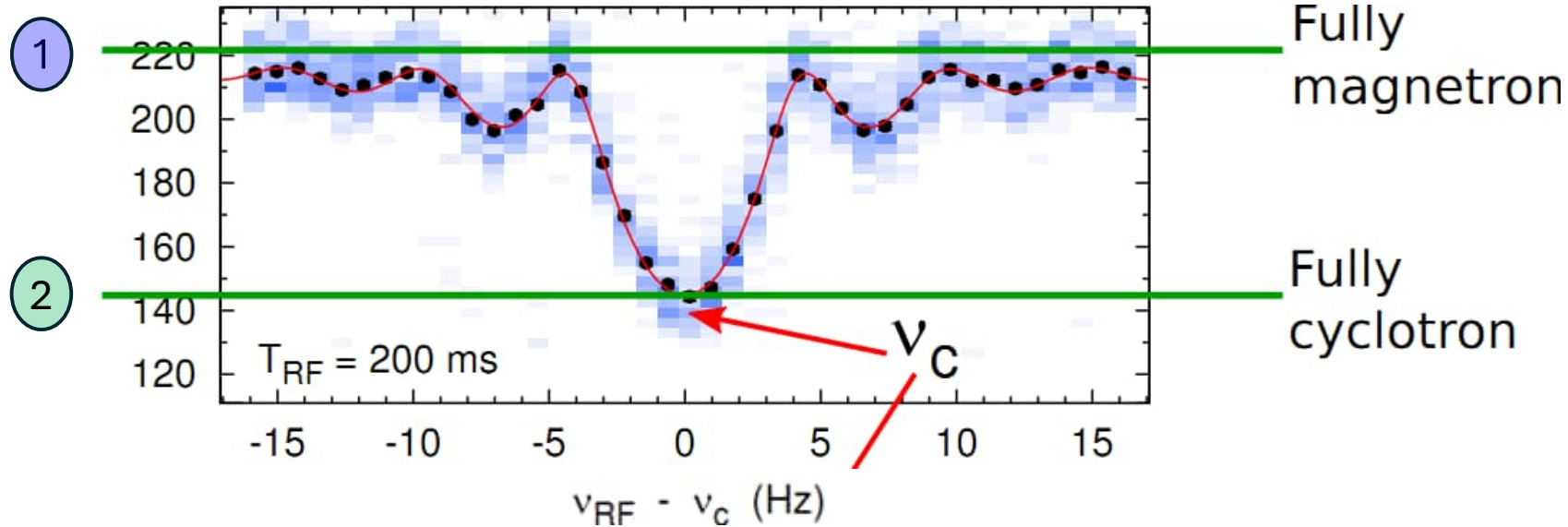
Basic idea

- Inject a bunch of ions into the trap, have them centred
- Excite ions to a well-defined radius of the magnetron motion (mass-independent)
- Apply a quadrupole excitation to convert the magnetron to the cyclotron motion (scan ν_{RF} over ions ν_c)
- Extract ions from the trap and record their TOF (start signal is ejection, ion's arrival is the stop signal)



$$\vec{F} = -\vec{\mu}(\vec{\nabla} \vec{B}) = -\frac{E_r}{B} \frac{\partial B}{\partial z} \hat{z}$$

Time-of-Flight Ion Cyclotron Resonance method



- 1 = off resonance
2 = on resonance

- Scanning: frequency-by-frequency; several ion bunches per point
- Blue shaded pixels:
 - Ions with this TOF
 - Denser color- more ions
- Black points (with error bar): average TOF for this frequency

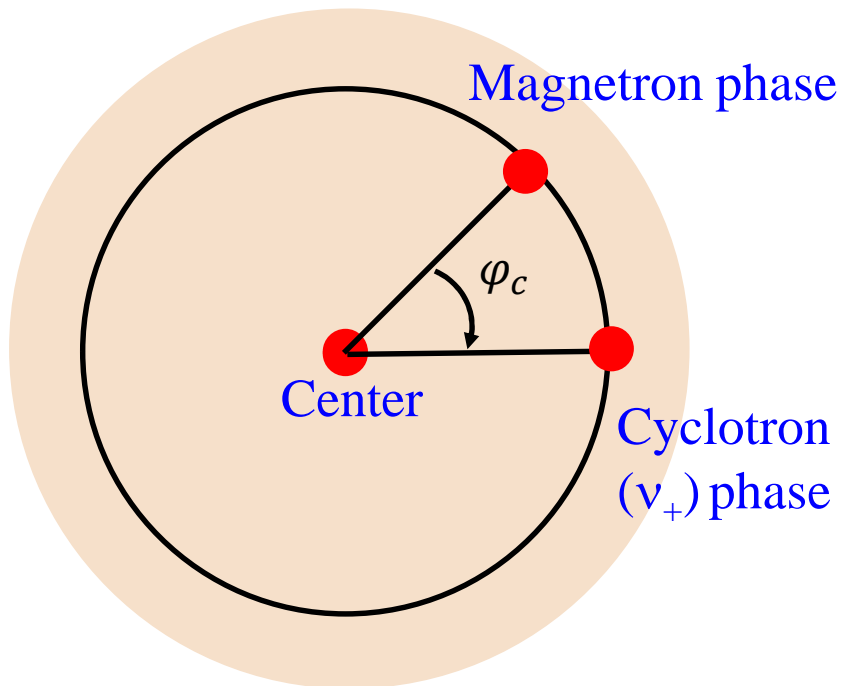
- Solid line is theoretically expected lineshape, mainly determined by the Fourier transform of the RF excitation profile.
- The width and thus resolving power is Fourier limited by the duration of the quadrupole excitation.

$$R = \frac{m}{\Delta m} = \frac{\nu_c}{\Delta \nu_c} \approx \nu_c T_{RF}$$

*M. König et al., *Int. J. Mass Spec. Ion Process.* 142 (1995) 95

Phase-Imaging Ion Cyclotron Resonance method

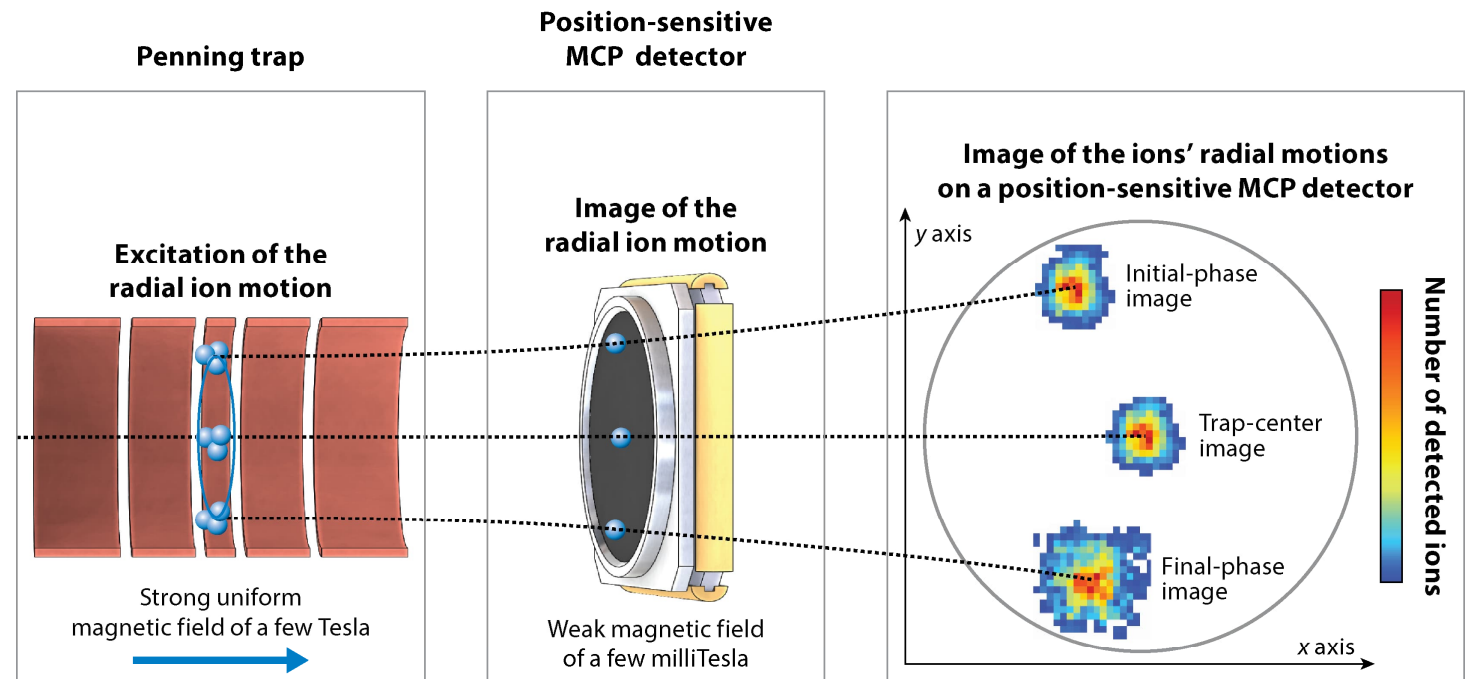
This is a method which has been developed in recent years...



$$\nu_c = \frac{\varphi_c + 2\pi n_c}{2\pi t}$$

S. Eliseev et al., Appl. Phys. B 114 (2014) 107
D.A. Nesterenko et al., Eur. Phys. J. A 54 (2018) 154

n_{\pm} = number of turns
 ϕ_{\pm} = phase of the radial frequency ν_{\pm}
 t = phase accumulation time



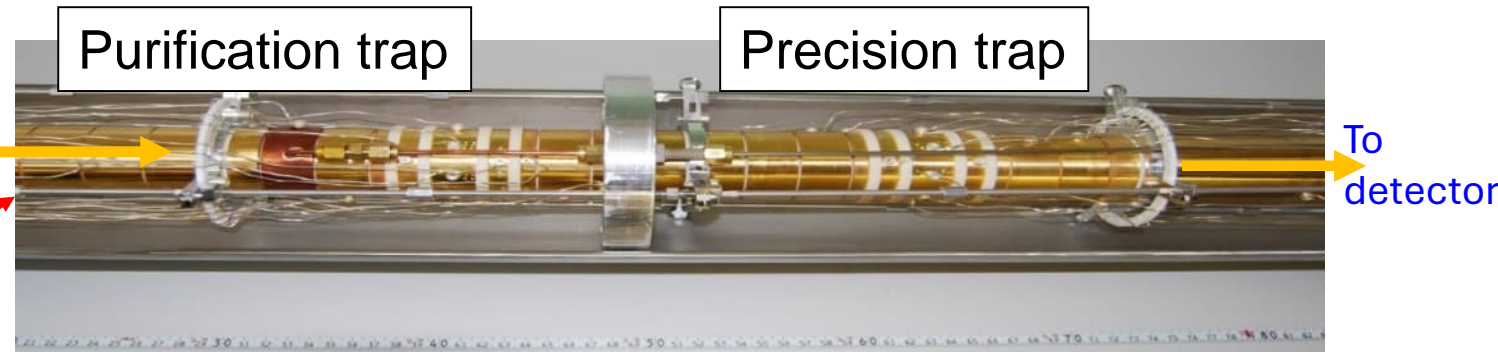
Dilling J, et al. 2018.
Annu. Rev. Nucl. Part. Sci. 68:45–74

J. Dilling et al., Annu. Rev. Nucl. Part. Sci. 68 (2018) 45

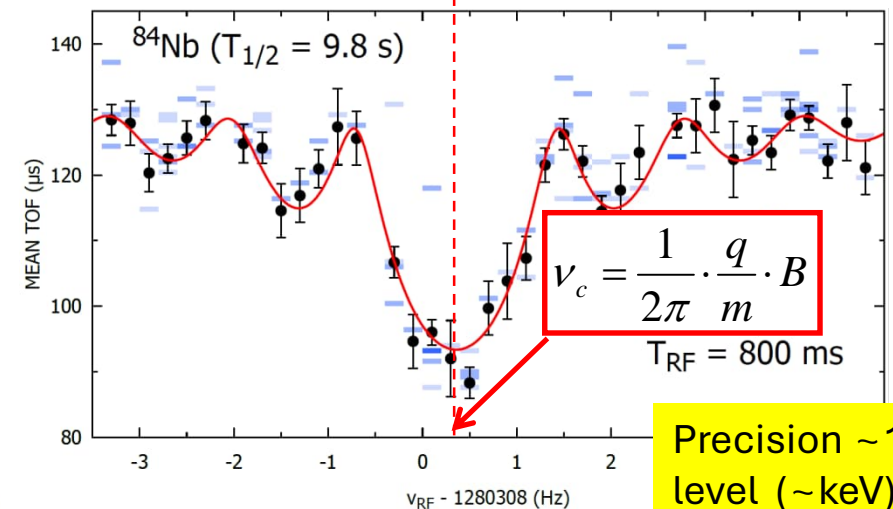
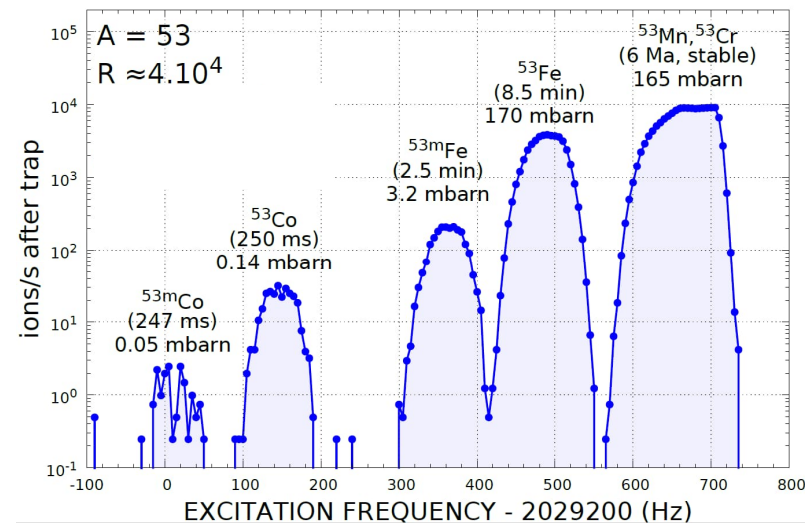
Offers a 5-fold gain in precision of the cyclotron-frequency determination, and 40-fold gain in resolving power.

The JYFLTRAP double Penning trap

- ❖ Homogeneous 7T B field
- ❖ 100V deep quadrupole potential
- ❖ Cylindrical geometry



Mass-selective buffer gas cooling*

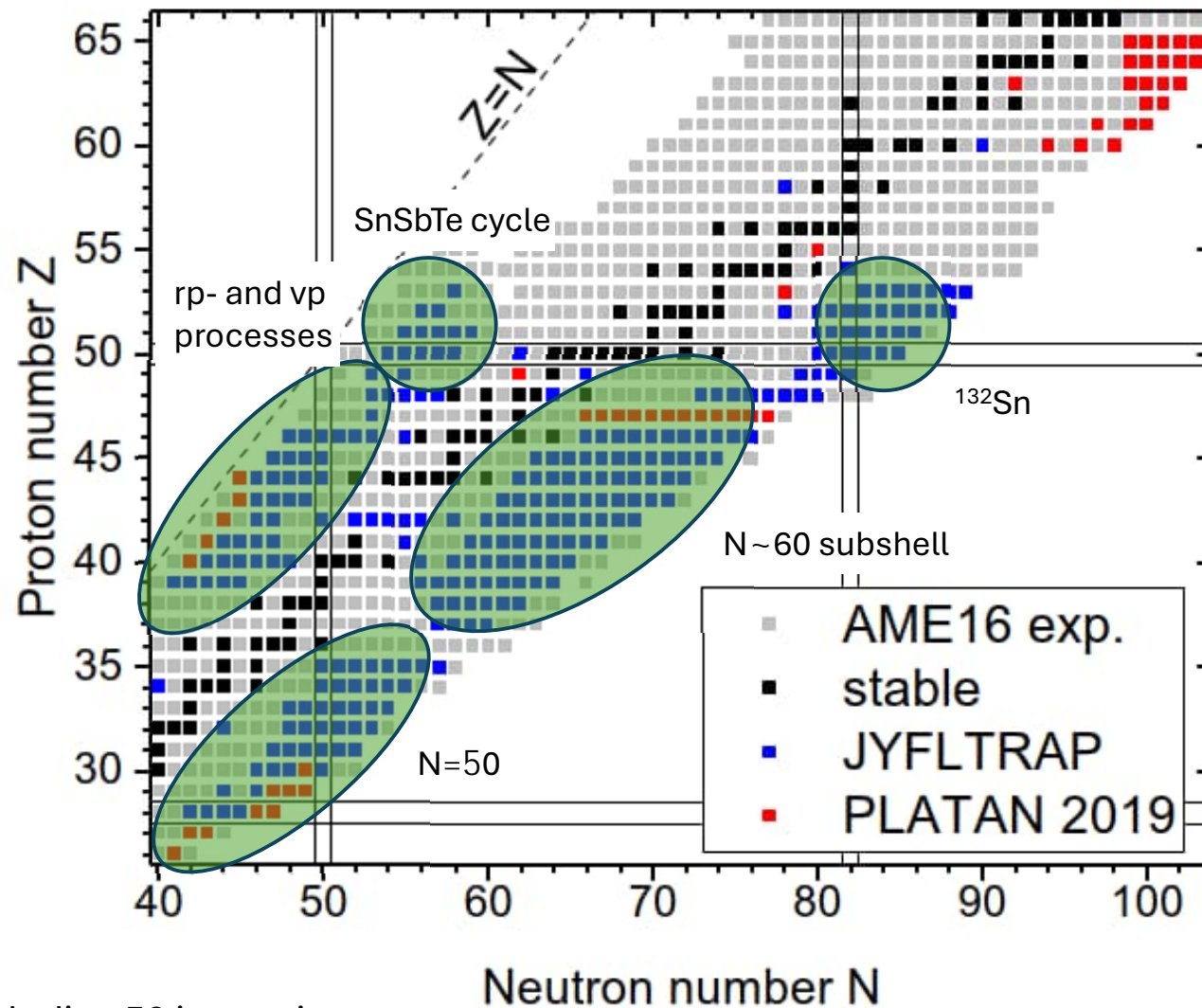


Precision $\sim 10^{-8}$ level ($\sim \text{keV}$)

*Savard et al., Phys. Lett. A 158, 247 (1991)

T. Eronen et al., Eur. Phys. J. A 48 (2012) 46

Mass harvesting at JYFLTRAP



>400 masses measured including 50 isomeric states

A. Kankainen, Hyp. Int. 241 (2020) 43

Trap-assisted decay spectroscopy

Nowadays, almost 60% of all JYFLTRAP Penning trap experiments are not for mass measurements, but for mass purification. The nuclear decay spectroscopy community relish having pure beams, sometimes even isomerically purified!

A=111 fission fragments

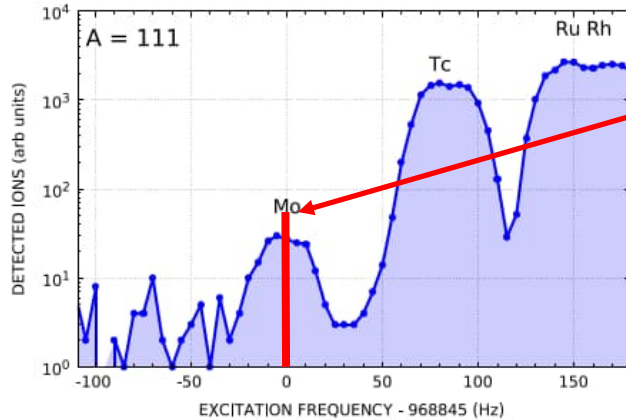
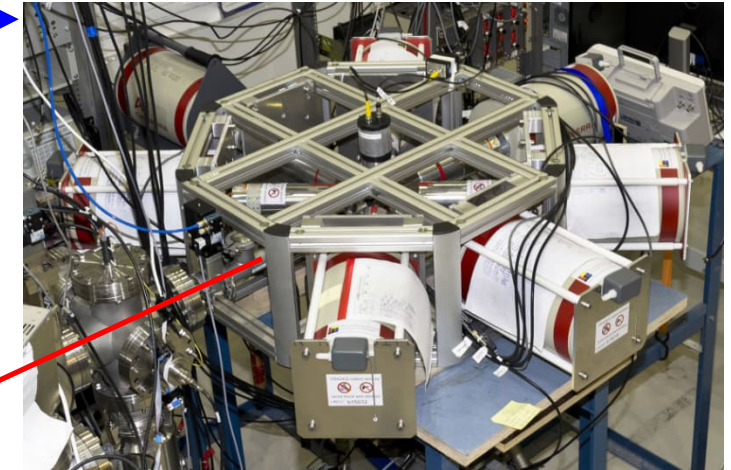
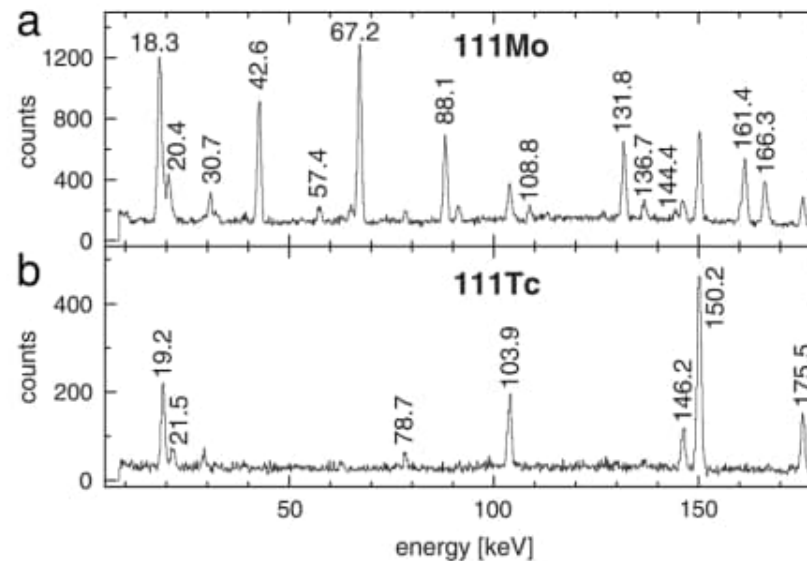
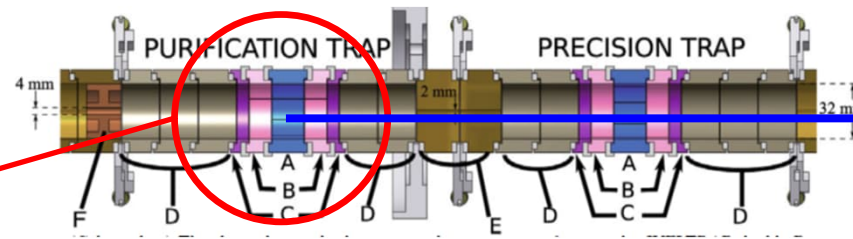


Fig. 24. Mass spectrum of A = 111 isobars.

- Monoisotopic beam of ¹¹¹Mo delivered downstream for post-trap decay spectroscopy.



Low-energy Ge array (U-Warsaw)

J. Kurpeta et al., Phys. Rev. C 84 (2011) 044304

Once upon a time we wanted to study
silver with lasers and traps

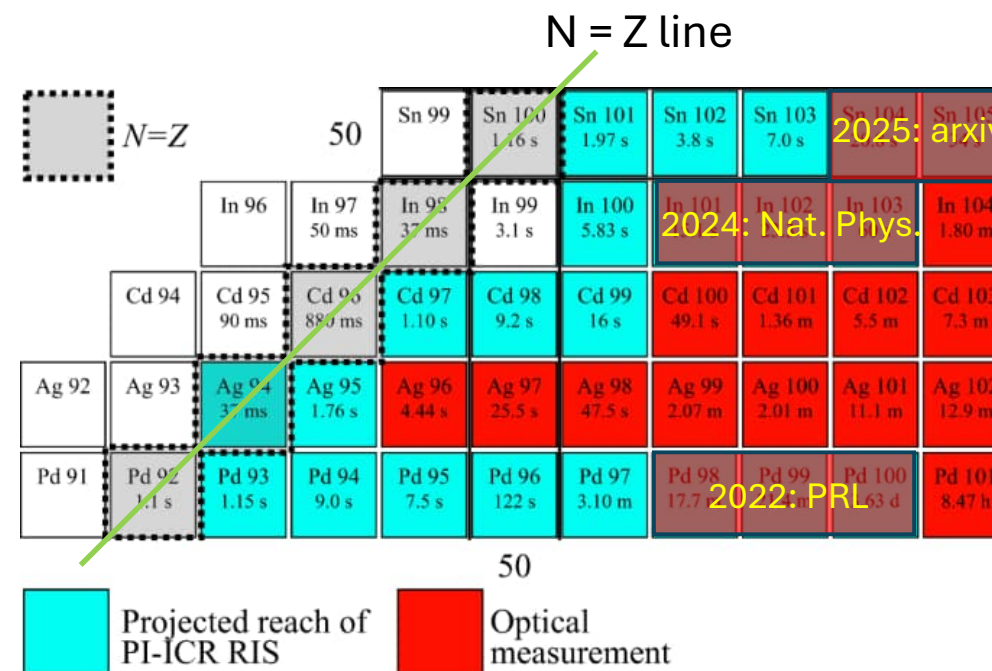


First we need some physics motivations

Nuclear structure trends

- Region below Sn ($Z = 50$) is of high interest – probing shell evolution below the closed proton shell ($Z = 50$) and between neutron shell closures at $N = 50$ and 82 (spanning 32 neutrons!)
- Data on neutron-rich odd-odd Ag isotopes is absent or incomplete
- Spin assignments are often tentative and in conflict due to experiments lacking isomeric or isobaric purification
- High precision mass and laser spectroscopy measurements can be combined with decay spectroscopy data to firmly establish spin and parity assignments, and level ordering.

Laser spectroscopy near ^{100}Sn



- Very neutron-poor isotopes are challenging to produce
- Reactions offer small cross section
- Often overwhelming contamination (same mass but closer to stability)

M. Reponen, R.P de Groote,...IM, et al., Nature Comm. 12 (2021) 4596

RIB methods to access the Ag isotopic chain

$N=Z$ ^{94}Ag (gs):
 $T_{1/2} = 26$ ms

Here we are going to focus on the neutron-deficient isotopes
(as it makes a nicer story!!)

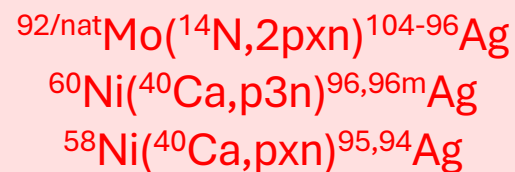
^{125}Ag : $T_{1/2}$
 $= 176$ ms

$N=50$

$N=82$



Heavy-ion fusion-evaporation reactions



Typical heavy-ion gas cell efficiency
~1%, few 100ms extraction time

Light-ion fusion-evaporation reactions



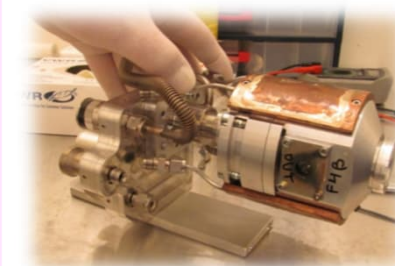
Light ion guide (gas cell)

Efficiency 1-10%

Proton-induced fission of U $^{113-125}\text{Ag}$

Fission ion guide
(gas cell)

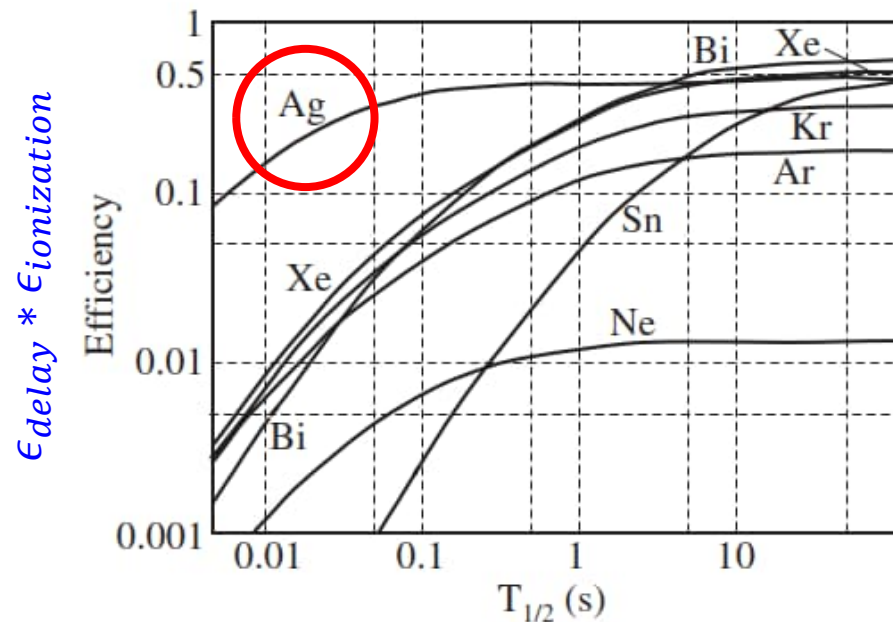
Typical efficiency
0.1%



Access to nuclei above $A = 125$ at ISOLDE; 1.4 GeV protons on UC_x target.

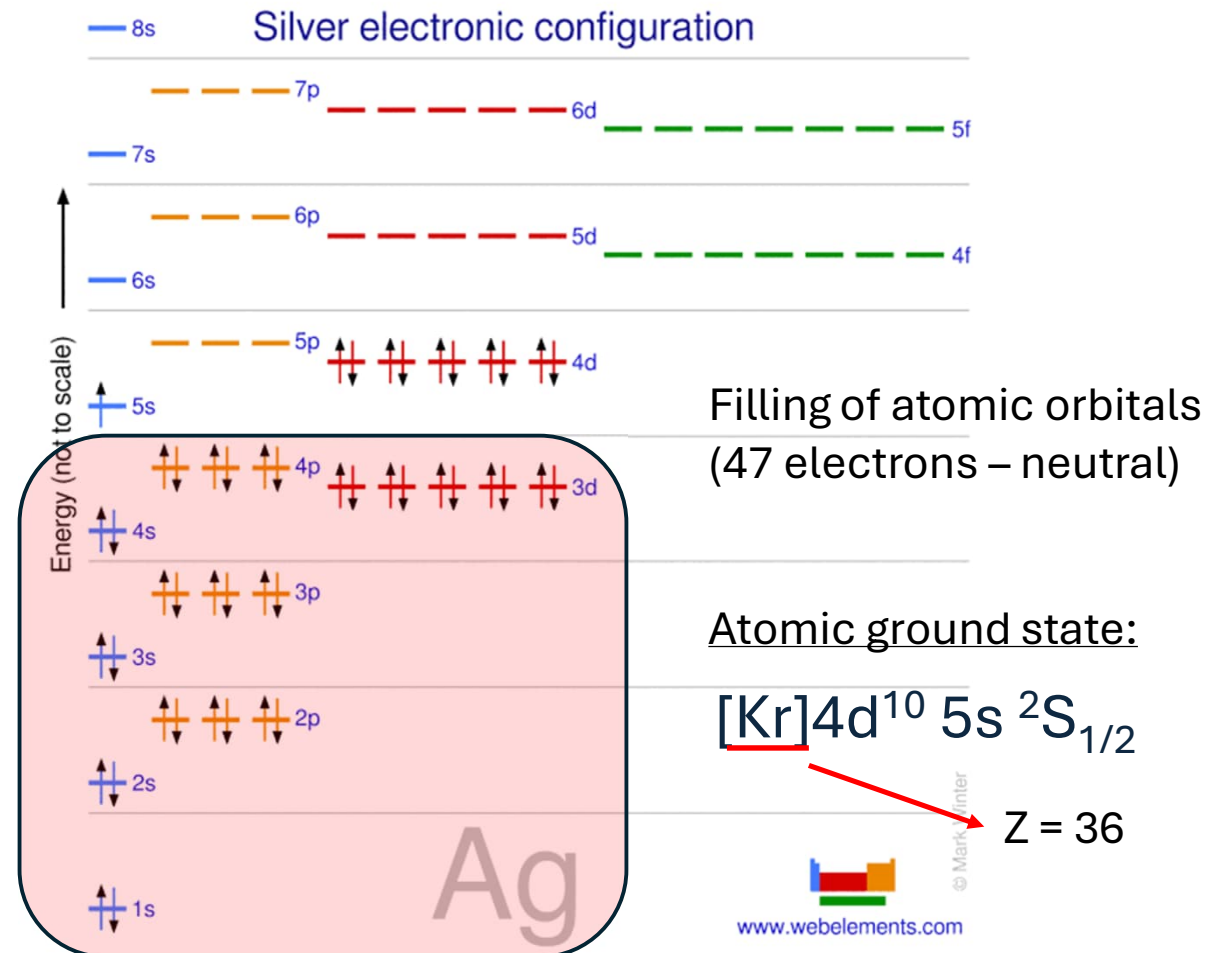
Recall from lecture 2 – FEBIAD ion source

- Alternative approach for the extraction of Ag was motivated by the FEBIAD ion source from the GSI on-line mass separator. Silver had an exceptional release from a graphite catcher, **tens of ms timescale and close to 50% extraction efficiency**.
- Selective and efficient laser ionization in a hot cavity.

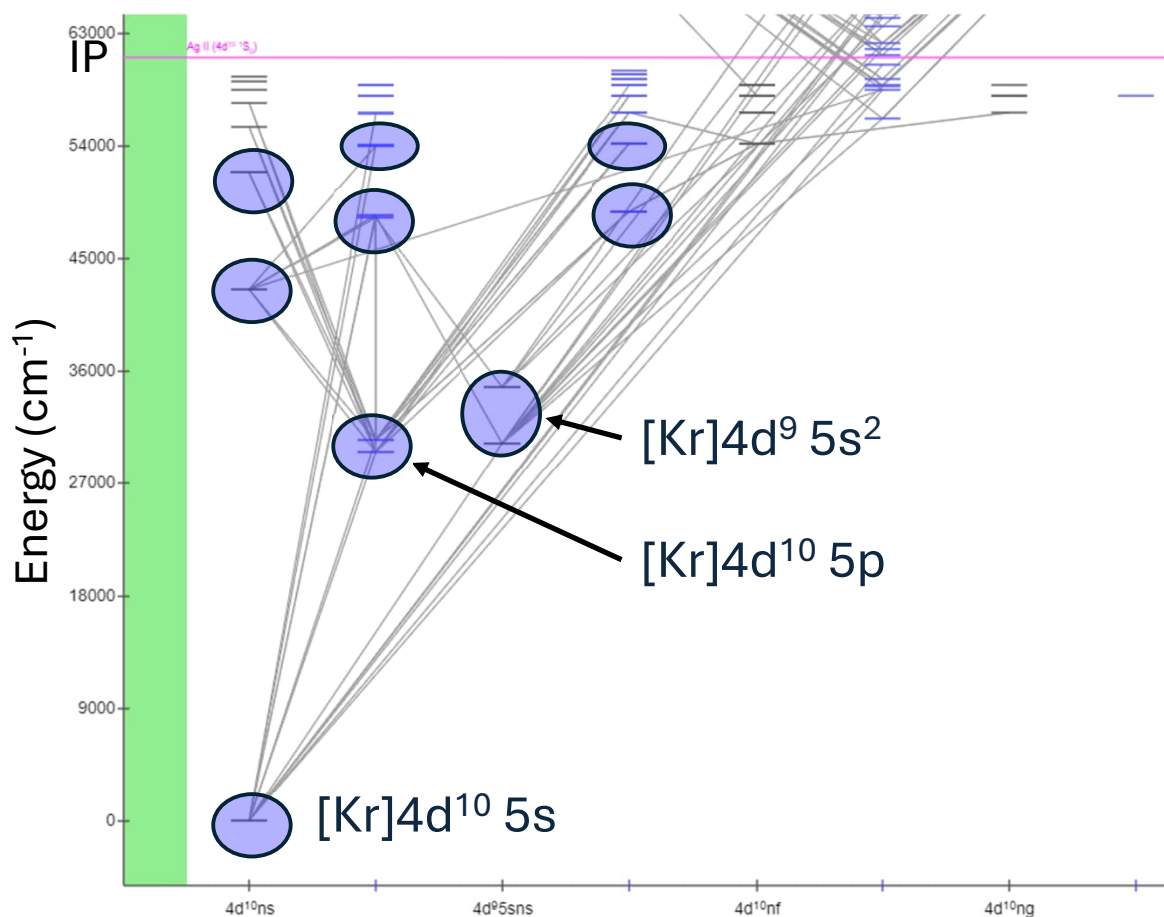


R. Kirchner et al., NIMB 70 (1992) 186

Silver (Z = 47) has very suitable atomic properties



Lines and levels of neutral Ag (Ag I)

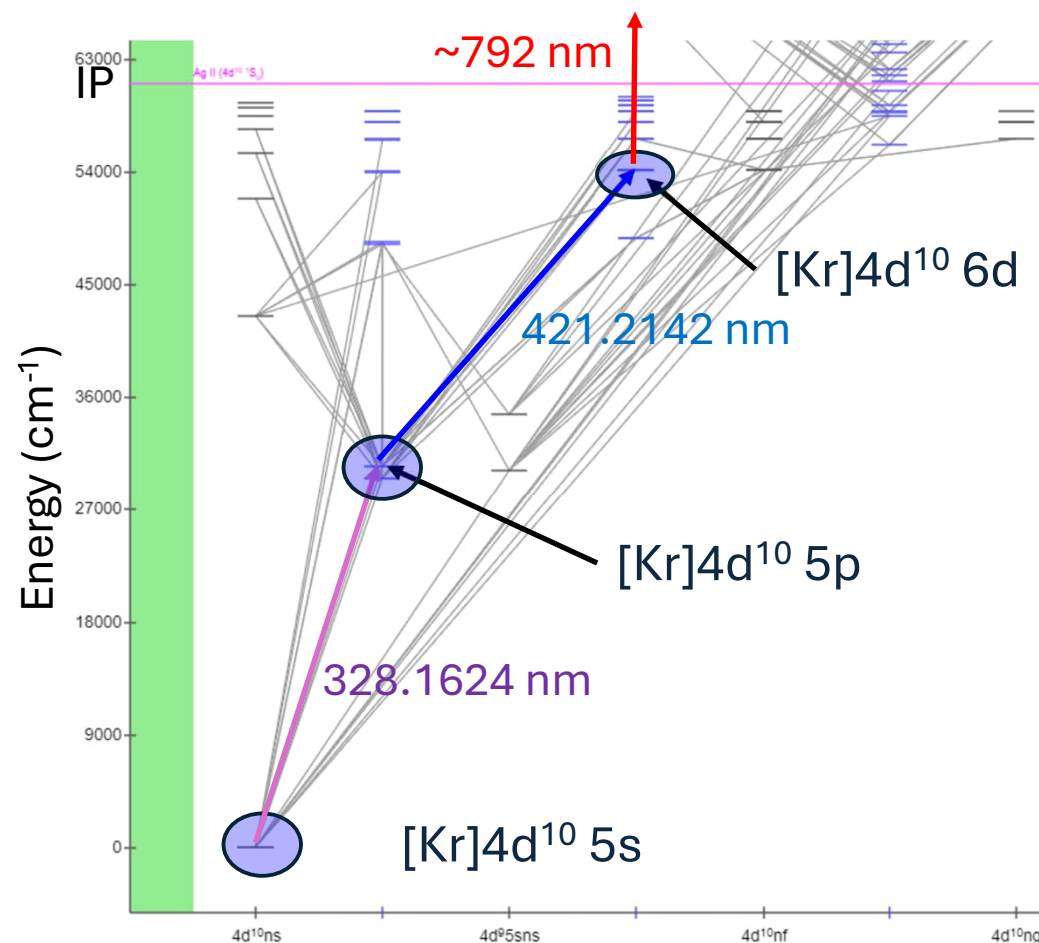


https://physics.nist.gov/PhysRefData/ASD/levels_form.html

Configuration	Term	J	Level (cm ⁻¹)	Uncertainty (cm ⁻¹)
4d ¹⁰ 5s	² S	1/2	0.000000	0
4d ¹⁰ 5p	² P°	1/2	29 552.05741	0.00014
		3/2	30 472.66516	0.00022
4d ⁹ 5s ²	² D	5/2	30 242.298349	0.000006
		3/2	34 714.22643	0.00010
4d ¹⁰ 6s	² S	1/2	42 556.147	0.001
4d ¹⁰ 6p	² P°	1/2	48 297.406	0.002
		3/2	48 500.8105	0.0004
4d ¹⁰ 5d	² D	3/2	48 743.969	0.002
		5/2	48 764.219	0.002
4d ¹⁰ 7s	² S	1/2	51 886.965	0.001
4d ¹⁰ 7p	² P°	1/2	54 041.037	0.002
		3/2	54 121.108	0.001
4d ¹⁰ 6d	² D	3/2	54 203.119	0.002
		5/2	54 213.564	0.003

- Filled atomic d shell
- Valence electron can be placed in 5s, 5p, 6s, 6p, ... to form the lowest-energy atomic states

Resonance ionization scheme



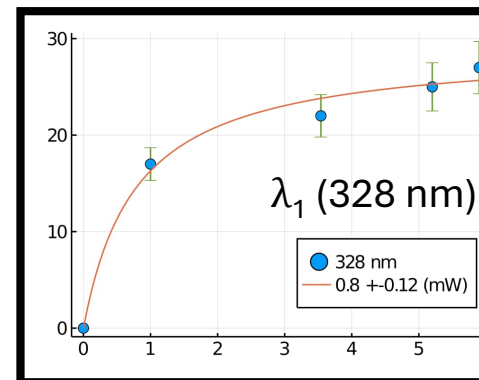
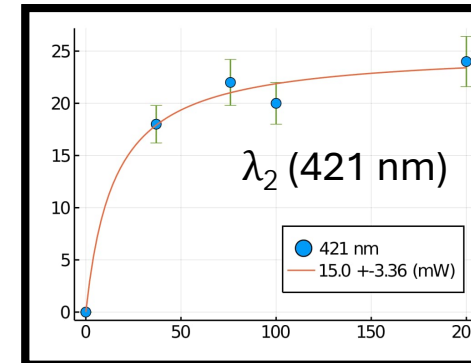
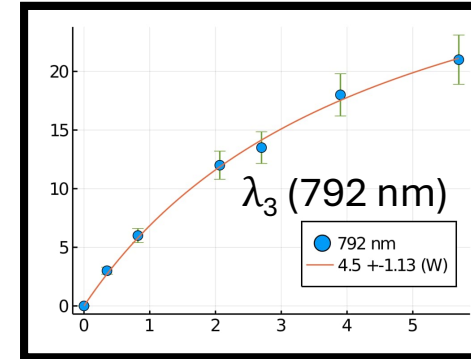
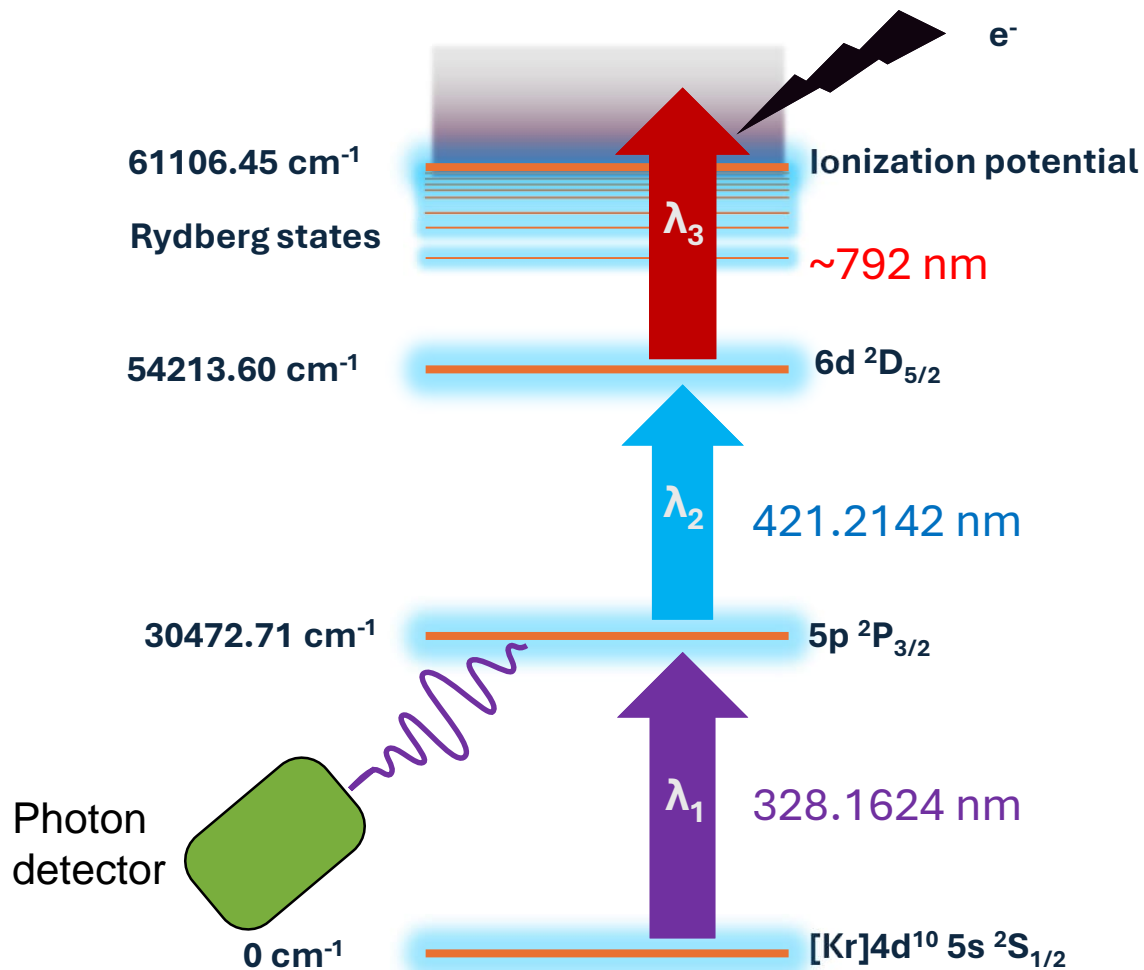
Configuration	Term	J	Level (cm ⁻¹)	Uncertainty (cm ⁻¹)
4d ¹⁰ 5s	² S	1/2	0.000000	0
4d ¹⁰ 5p	² P°	1/2	29 552.05741	0.00014
		3/2	30 472.66516	0.00022
4d ⁹ 5s ²	² D	5/2	30 242.298349	0.000006
		3/2	34 714.22643	0.00010
4d ¹⁰ 6s	² S	1/2	42 556.147	0.001
4d ¹⁰ 6p	² P°	1/2	48 297.406	0.002
		3/2	48 500.8105	0.0004
4d ¹⁰ 5d	² D	3/2	48 743.969	0.002
		5/2	48 764.219	0.002
4d ¹⁰ 7s	² S	1/2	51 886.965	0.001
4d ¹⁰ 7p	² P°	1/2	54 041.037	0.002
		3/2	54 121.108	0.001
4d ¹⁰ 6d	² D	3/2	54 203.119	0.002
		5/2	54 213.564	0.003

$$J_1 = \frac{1}{2} \rightarrow J_2 = \frac{3}{2} \rightarrow J_3 = \frac{5}{2}$$

- Ground state with J = 1/2 has sensitivity to magnetic dipole moment
- Excited state with J = 3/2, additional sensitivity to Q_s

Checking the saturation of the scheme

Ag laser ionization scheme



- We also measure the laser powers for each step at the end of the optical table and entering the transfer tube of the hot cavity.
- Typical transport efficiency (April 2025):
 - λ_1 = 50%
 - λ_2 = 30%
 - λ_3 = 60%
- We optimize the laser power with respect to ion count rate and spectral resolution (in-source)

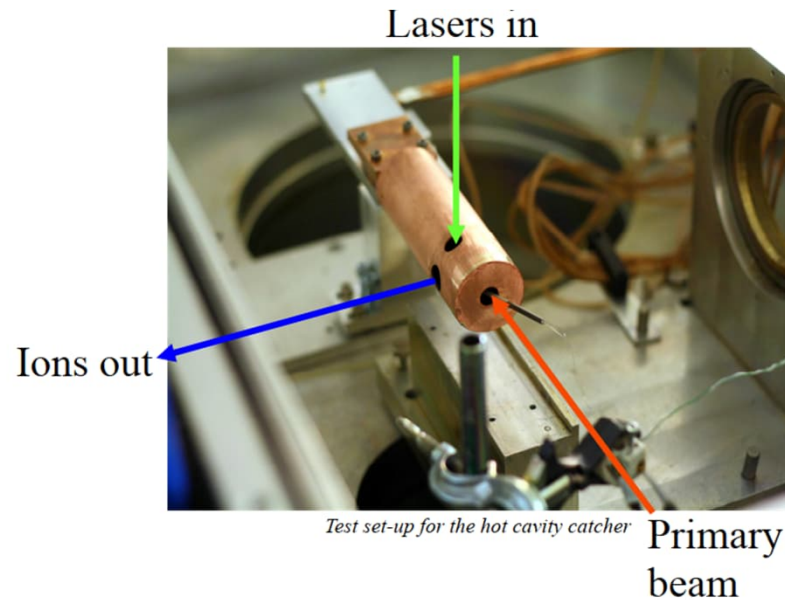
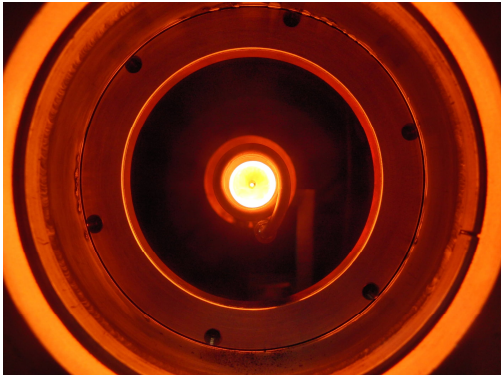
A few small iterations in the hot cavity design

- In fact version 0 started way back in 2007!!

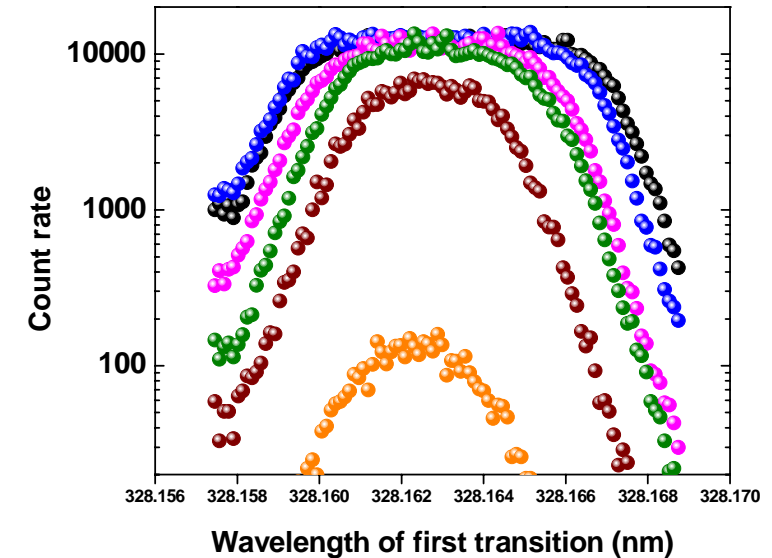


Version 1

- Two FEBIAD ion sources from GSI (2008-2009)
- Unstable operation
- Melted components
- First offline RIS results!



First step wavelength scan vs oven temp

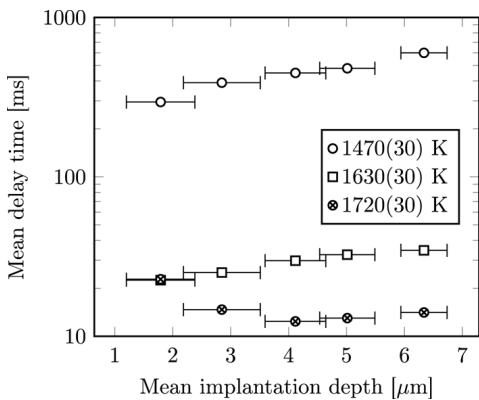
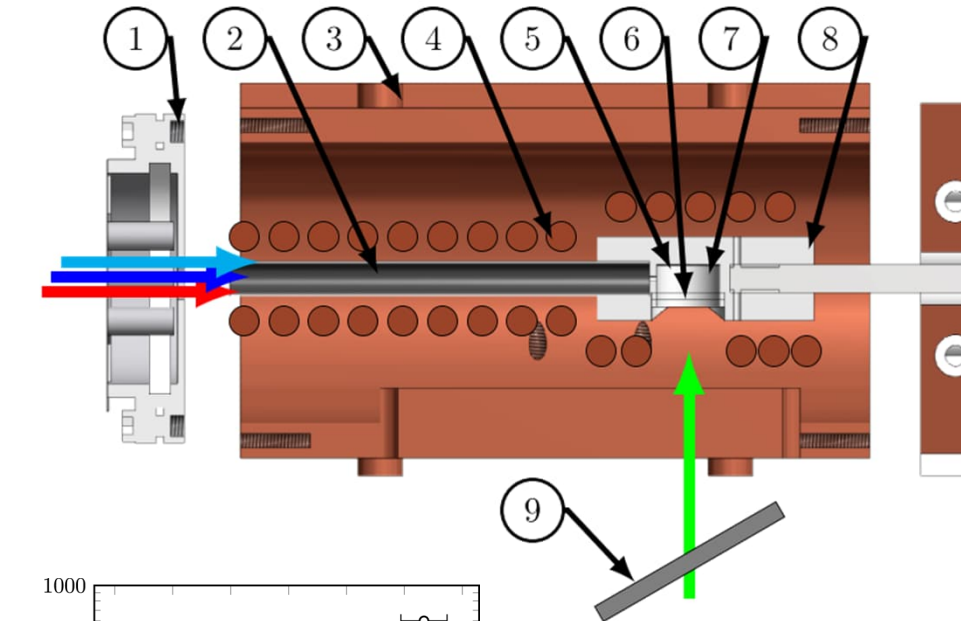


M. Reponen...IM et al., Eur. Phys. J A 42 (2009) 509

Version 2

- Development of RF heating mechanism with JYFL ECR ion source team
- No specific laser interaction region
- Huge energy spread
- Poor efficiency

A few small iterations in the hot cavity design

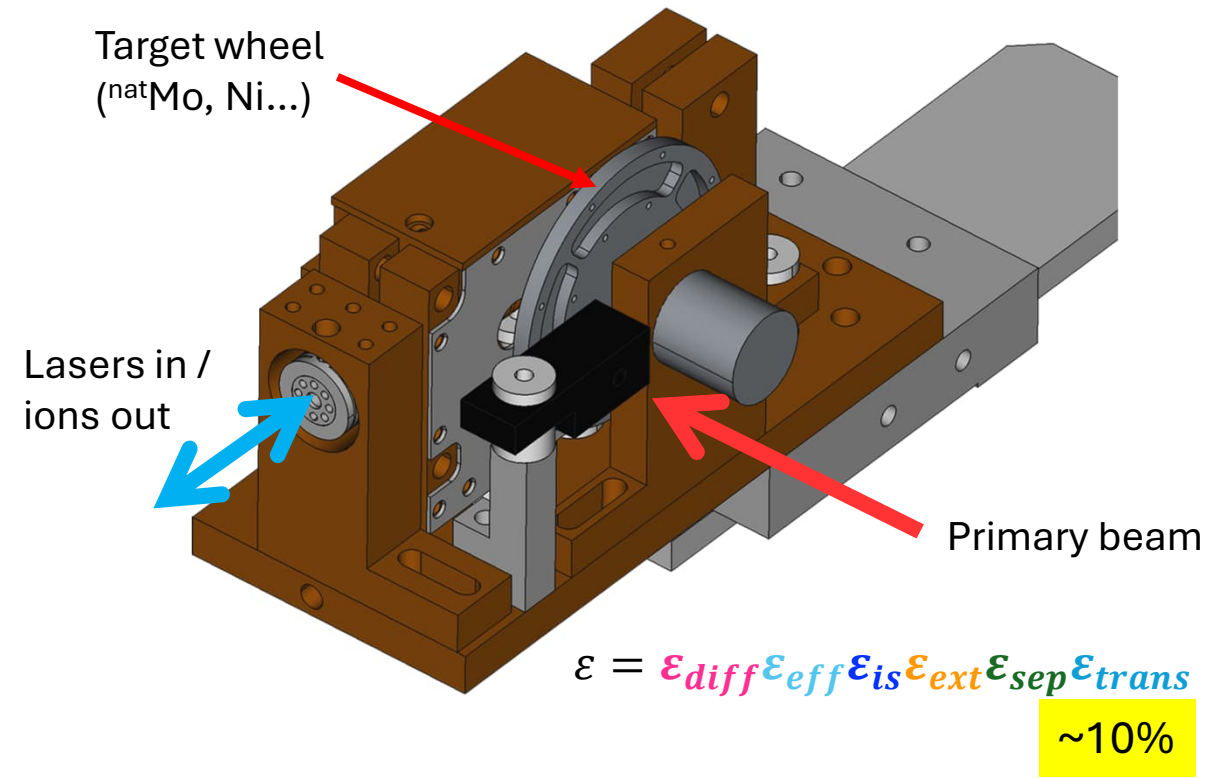


Version 3

- Included a transfer tube for laser ionization – inductively heated
- Demonstrated fast extraction of (implanted) silver

Version 4

- Separate heating mechanisms for the catcher & transfer tube
- Sigradur tubes (glassy carbon)
- First extraction of radioactive ^{99}Ag (half-life 124 s); γ -ray detection

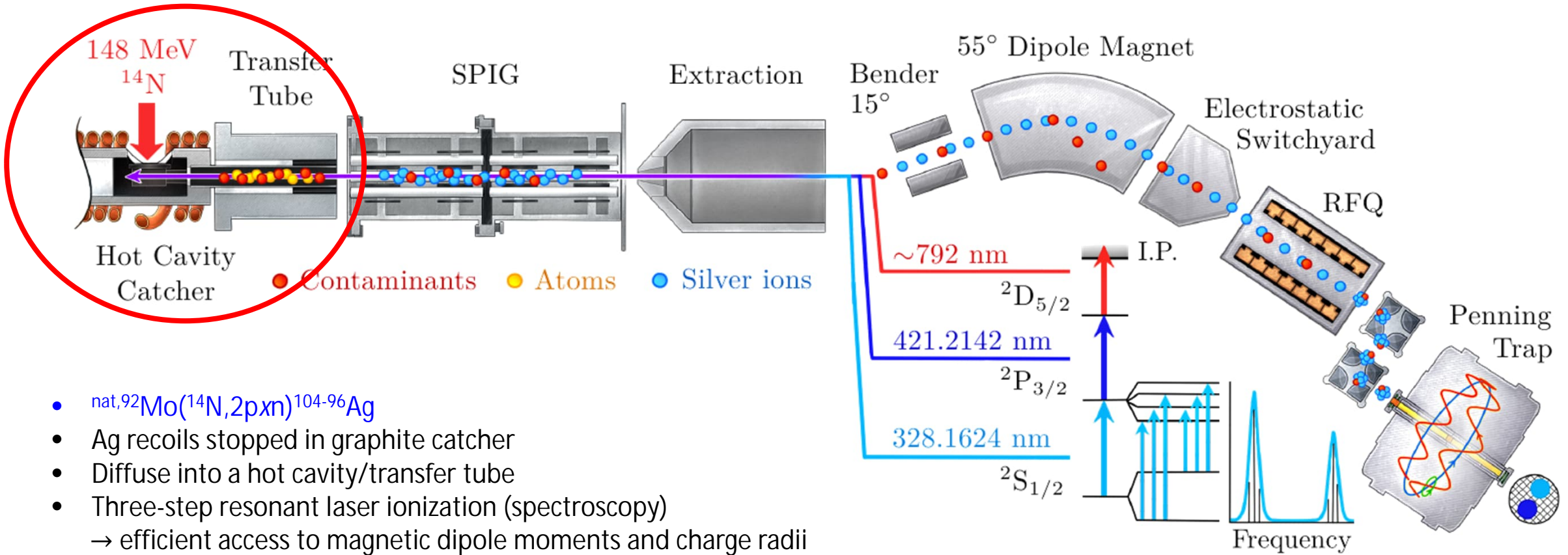


M. Reponen, I.M et al., Rev. Sci. Instrum. 86 (205) 123501

...and then we worked on improving the ion detection...

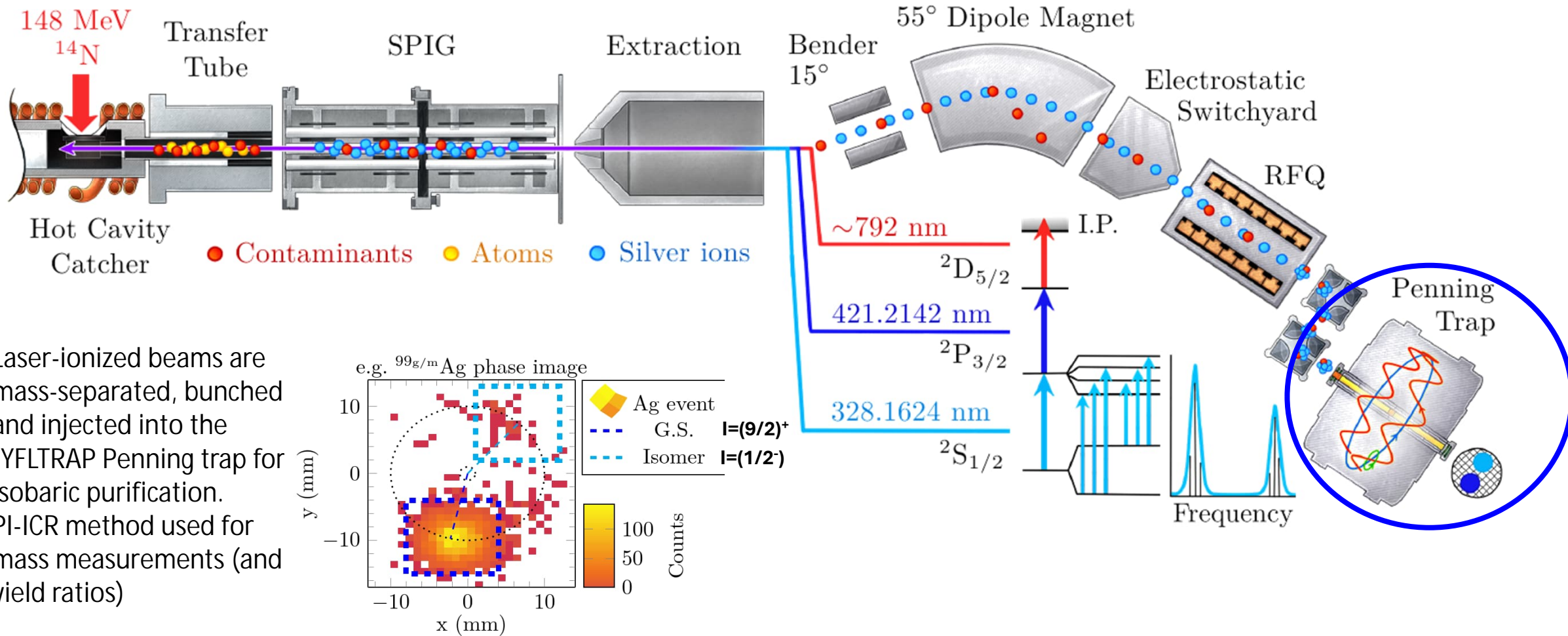
Penning trap-assisted in-source spectroscopy

Recent efforts combining methods from ion manipulation and trapping techniques with laser resonance ionization have enabled almost a complete suppression of background, opening a window to the most exotic nuclei.



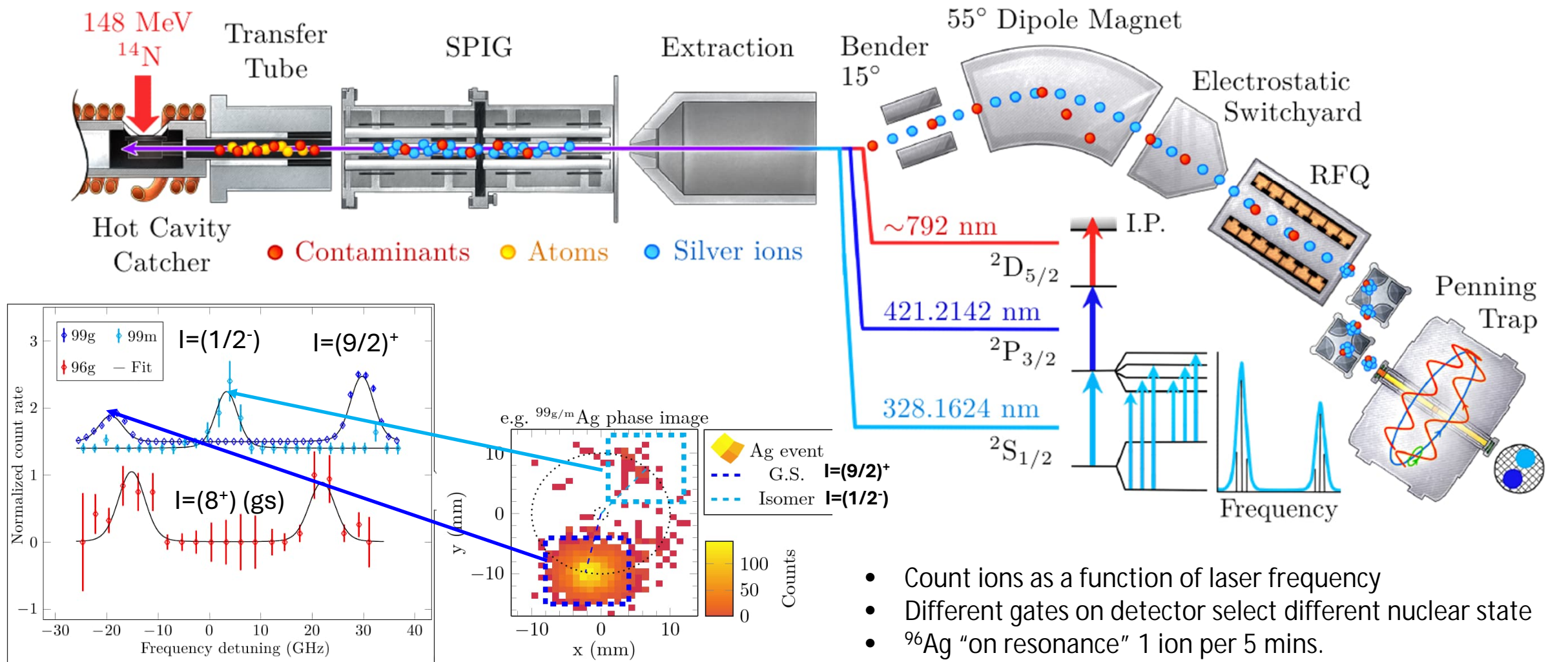
- $\text{nat},^{92}\text{Mo}(^{14}\text{N},2\text{pxn})^{104-96}\text{Ag}$
- Ag recoils stopped in graphite catcher
- Diffuse into a hot cavity/transfer tube
- Three-step resonant laser ionization (spectroscopy)
→ efficient access to magnetic dipole moments and charge radii

Penning trap-assisted in-source spectroscopy



- Laser-ionized beams are mass-separated, bunched and injected into the JYFLTRAP Penning trap for isobaric purification.
- PI-ICR method used for mass measurements (and yield ratios)

Penning trap-assisted in-source spectroscopy



- Count ions as a function of laser frequency
- Different gates on detector select different nuclear state
- ^{96}Ag "on resonance" 1 ion per 5 mins.
- Further improvement of ^{96}Ag yield to 1 ion per 25 seconds

M. Reponen et al., Nature Comm. 12 (2021) 4596

Evolution of charge radii across $N = 50$

Recall Lecture 1:

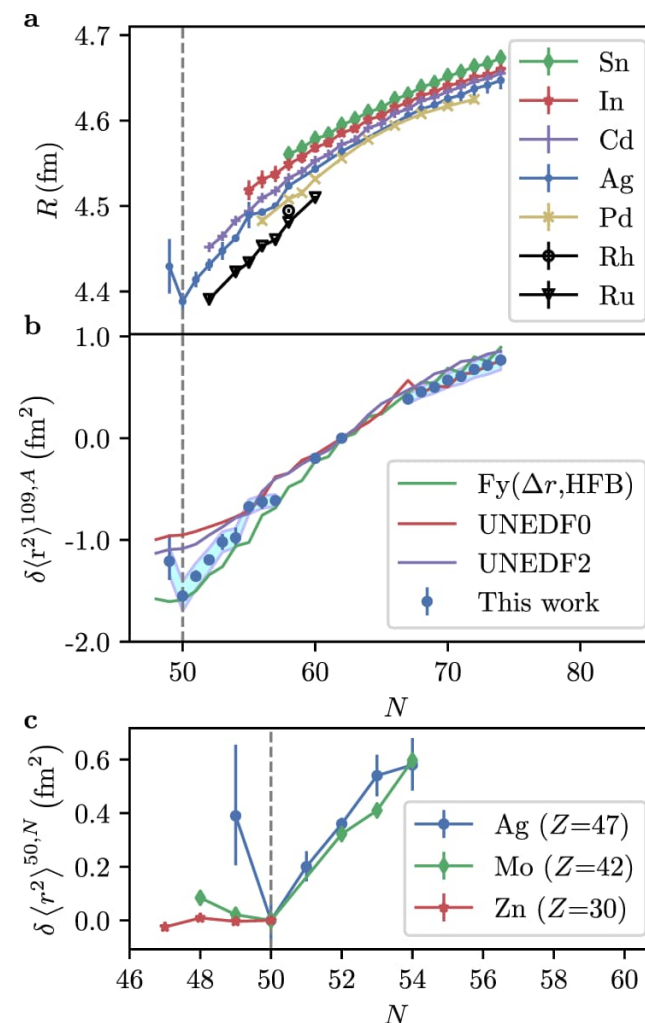
$$\delta\nu_i^{A,A'} = \overset{\text{Mass shift}}{M_i \frac{A' - A}{AA'}} + \overset{\text{Field shift}}{F_i \delta\langle r^2 \rangle^{A,A'}}$$

THEORY

- A King plot evaluation would be possible if independent radius data (for Ag) is available for at least three different isotopes.
- Ag has only two stable isotopes ($A = 107, 109$)

Atomic factors F and M from empirical estimation:

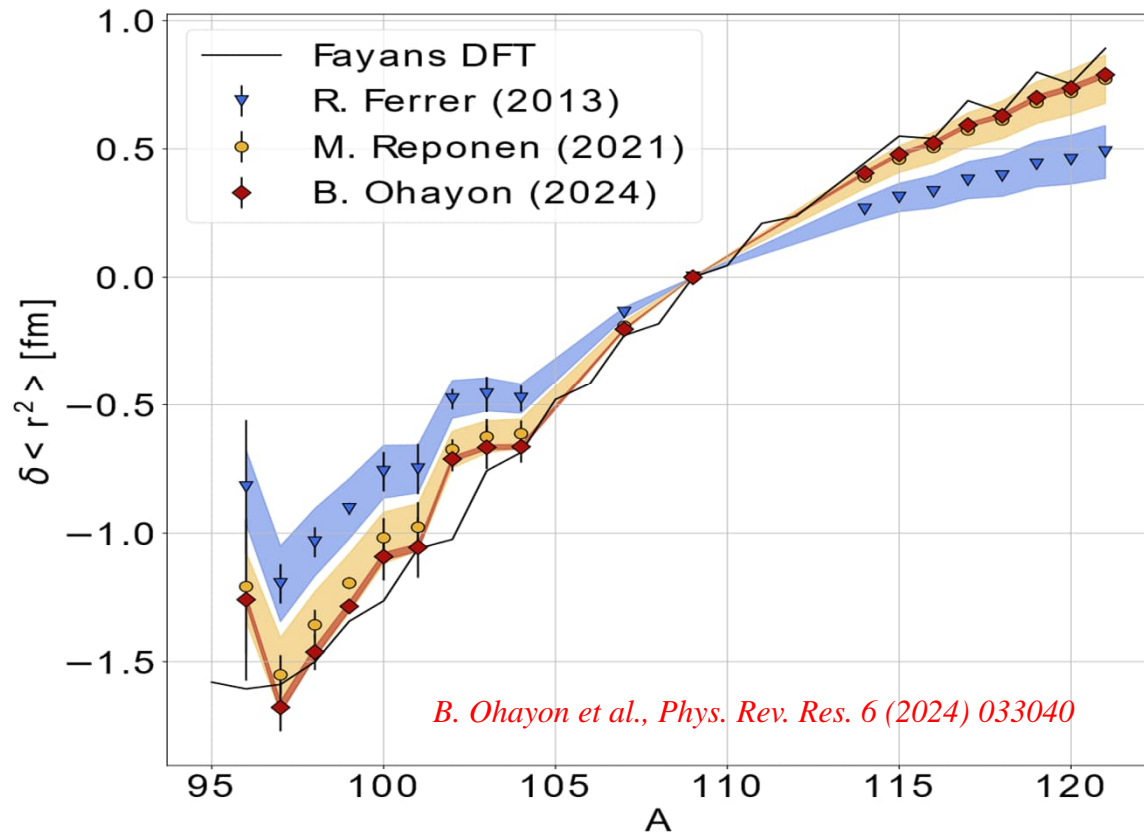
$$F = -4300(300) \text{ MHz fm}^{-2}, M = 1956(360) \text{ GHz u}$$



- Measurements cross $N=50$ shell closure in the region of ^{100}Sn for the first time.
- Energy density functionals (UNEDF) predict a rather smooth behaviour; Fayans EDF better reproduces local variations.
- None of the models reproduces the remarkably sharp increase in crossing $N=50$.

M. Reponen et al., Nature Comm. 12 (2021) 4596

Implication of recent *ab initio* calculations

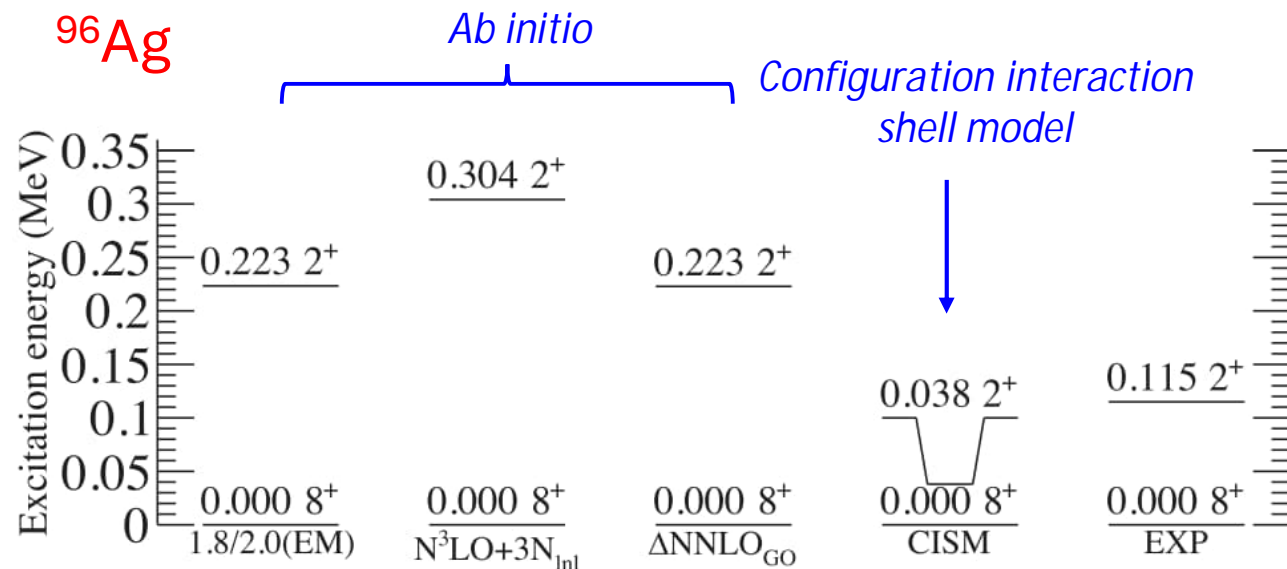


Note the improvement in the uncertainties of the atomic factors (often dominating the extracted charge radii).

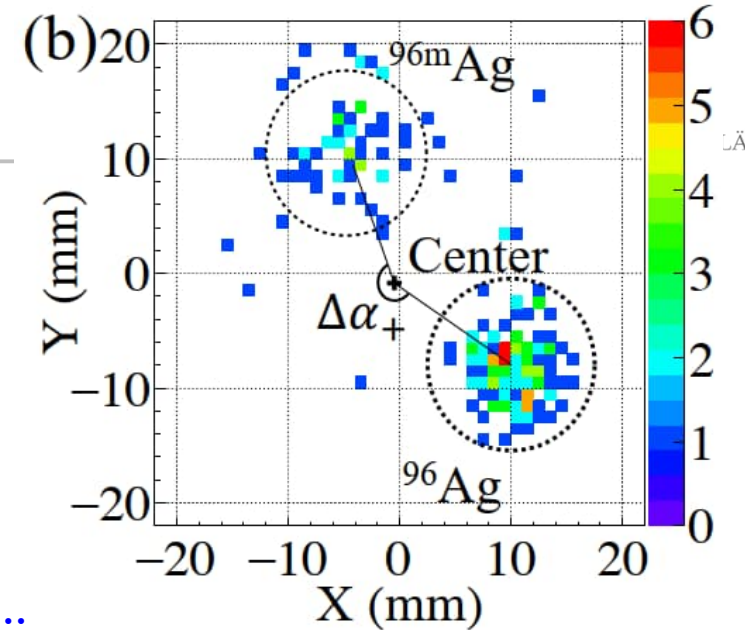
- Ferrer (2013); in-gas cell RIS of Ag on 328-nm line. Atomic factors F and M from empirical estimation:
 - $F = -4300(300) \text{ MHz fm}^{-2}$, $M = 821(450) \text{ GHz u}$
- Reponen (2021); in-source hot cavity on 328 nm line. Atomic factors F and M from empirical estimation:
 - $F = -4300(300) \text{ MHz fm}^{-2}$, $M = 1956(360) \text{ GHz u}$
- Ohayon (2024); analytical response relativistic coupled cluster theory
 - $F = -3557(49) \text{ MHz fm}^{-2}$, $M = 1479(14) \text{ GHz u}$
- Skripnikov (2025); somewhat similar calculations to Ohayon
 - $F = -3634(44) \text{ MHz fm}^{-2}$, $M = 1318(46) \text{ GHz u}$

Mass measurements beyond $N = 50$

- Probing the robustness of the $N = 50$ shell closure via changes in the slope of S_{2n} (two-neutron empirical shell gap)
- Atomic masses of two β -decaying states identified in ^{96}Ag and measured for the first time
- Atomic mass of ^{95}Ag measured for the first time



Z. Ge et al., Phys. Rev. Lett. 133 (2024) 132503



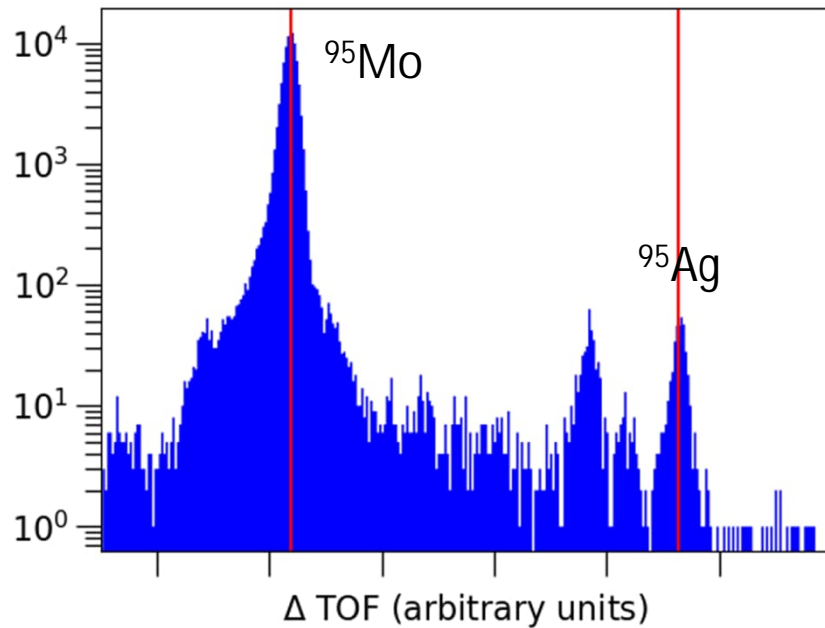
...and in 2023...



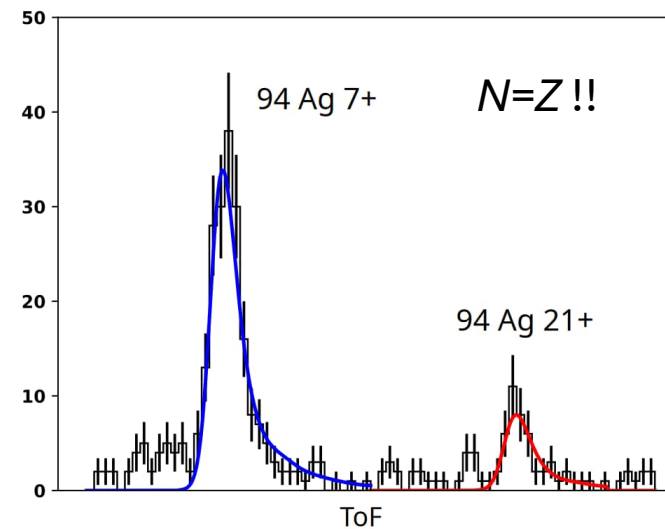
MR-TOF Mass Spectrometry of $N = Z$ ^{94}Ag

- The reliability of the MR-TOF method was verified with ^{94}Zr and ^{95}Ag (the latter measured at JYFLTRAP to 1.4 keV)
- We also measured the mass of $^{93}\text{Pd}^*$ (as well as $N = Z$ $^{92}\text{Pd}!!$)

**also measured with the FRS Ion Catcher at GSI*



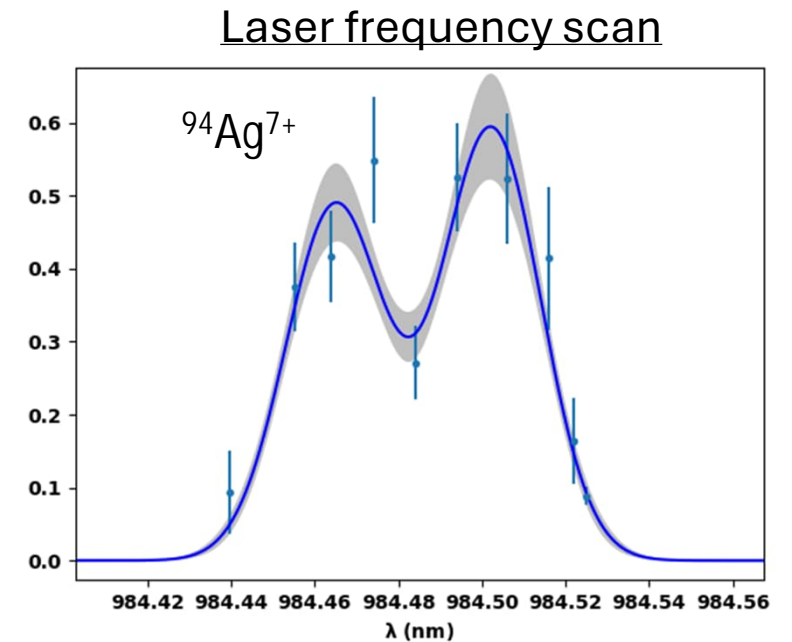
Mass precision of ^{95}Ag ~ 10 keV



Ion rates

- (7^+) = 0.55 ions/min
- (21^+) = 0.15 ions/min

Mass precision of $^{94}\text{Ag}^{21+}$ ~ 90 keV



V. Virtanen et al., to be submitted to Nature

Take home messages and summary

- Many experiments require cooled and bunched beams. RF cooler-bunchers are a staple diet of almost all RIB facilities.
- Mass spectrometry can take many forms, from MR-TOF devices, to Penning traps and also storage rings (the latter not discussed). There is no single ‘magic’ technique that can be considered optimal for the entire range of mass measurement uncertainties and nuclide half-lives.
- Nowadays, the most versatile and powerful techniques for the study of exotic nuclear ground state structure (masses, charge radii, moments & spins) combines all the methods we have been discussing. Selectivity, sensitivity and efficiency...we are now performing measurements at the extremes of exoticity. And these tools can also be combined with decay spectroscopy stations for laser-assisted, trap-assisted decay spectroscopy 😊.
- The experimental results go hand-in-hand with benchmarking theoretical methods.